Optimisation of radionuclide therapy by reduction of normal tissue damage

–^{177}Lu-octreotate therapy combined with α_1-microglobulin

Charlotte Andersson

Department of Medical Radiation Sciences
Institute of Clinical Science
Sahlgrenska Academy
University of Gothenburg

Gothenburg, Sweden, 2022

UNIVERSITY OF GOTHENBURG

Cover illustration by Charlotte Andersson, created with BioRender.com and worditout.com

Optimisation of radionuclide therapy
by reduction of normal tissue damage
^{177}Lu-octreotate therapy combined with α_1-microglobulin

Charlotte.andersson@gu.se

ISBN 978-91-8009-795-6

Printed in Borås, Sweden 2022
Stema Specialtryck AB

“Ett fel närmare rätt ett sätt att se på saken“
– Den Svenska Björnstammen

Abstract

^{177}Lu-octreotate is a radiopharmaceutical that is used to treat patients with somatostatin receptor (SSTR) expressing neuroendocrine tumours (NETs). Patients with NETs usually have spread disease at diagnosis, and treatment with ^{177}Lu-octreotate can offer a prolonged life and better quality of life, but is today seldom a cure for these patients. Radionuclide therapy is limited by the risk of side effects on the normal tissue, and in ^{177}Lu-octreotate treatment the kidneys and bone marrow are the main dose limiting organs. Optimisation of ^{177}Lu-octreotate therapy can be achieved by reducing the risk of radiation induced damage in kidneys and bone marrow, enabling higher administered activity. One proposed option is co-administration with the antioxidant α_1-microglobulin (A1M).

The overall purpose of this thesis was to investigate the possibility to optimise ^{177}Lu-octreotate therapy by reducing the radiation effects in normal tissues using A1M. More specifically the aims were 1) to investigate if co-administration with A1M results in a negative (protective) effect on the tumour response to ^{177}Lu-octreotate 2) to study the normal tissue response in mice following ^{177}Lu-octreotate administration with or without A1M and A1M alone, 3) and to propose biomarkers for ^{177}Lu-octreotate induced kidney damage.

Biodistribution of ^{177}Lu was investigated in BALB/c nude mice bearing human GOT2 NET after injection of ^{177}Lu-octreotate with or without A1M. Therapeutic effects were studied on human GOT1 NET in BALB/c nude mice after injection of ^{177}Lu-octreotate with or without A1M and A1M alone. Tumour volume was measured over time and regulation of apoptosis related genes was investigated after 1 and 7 days. Effects on normal tissues were studied in C57BL/6N mice injected with ^{177}Lu-octreotate with or without A1M and A1M alone. Early proteomic responses were investigated in kidney tissues and bone marrow at 1 and 7 days after injection. Regulation of apoptosis related genes was also investigated in kidney tissues at these time points. Late effects on kidneys were studied based on expression of proposed markers for kidney damage and proposed urinary biomarker levels. Findings were correlated with morphological signs of kidney injury.

No significant impact of A1M were observed on the therapeutic effects of ^{177}Lu-octreotate in NET. Findings includes no change in biodistribution of ^{177}Lu, no negative effect on tumour volume changes, and no general differences in regulation of apoptosis related genes when ^{177}Lu-octreotate was combined with A1M. A tissue-dependent early proteomic response was observed in kidney tissue, including regulation of previously observed radiation responsive proteins. No clear changes in regulation of these radiation-induced proteins was observed after co-administration of A1M. Regulation of pro- and anti-apoptotic genes was observed in kidney cortex and kidney medulla following ^{177}Lu-octreotate exposure. Indication of an A1M initiated pro-survival response was observed in kidney medulla when ^{177}Lu-octreotate was combined with A1M. Promising results were found for KIM-1, CDKN1A and S100A6 as biomarkers for ^{177}Lu-octreotate induced late kidney injury, and RBP4 as an early responding urinary biomarker. No clear protective effect of A1M on late radiation induced effects on kidneys were observed.

Keywords

Neuroendocrine tumours, kidney, bone marrow, proteomics, gene expression, apoptosis, biomarkers, radioprotector

Sammanfattning

Cancer är idag fortfarande en av de vanligare dödsorsakerna i Sverige (25%). Framsteg inom cancerforskning har lett till ökad överlevnad och många cancersjukdomar som förr innebar en säker död kan vi nu bota. Fortfarande är vissa cancertyper svåra att bota, särskilt i de fall när cancern är spridd i kroppen. Då är det svårt att avlägsna all tumörvävnad med operation eller vanlig strålbehandling. Behandling med radioaktiva läkemedel har visat sig vara användbart för många av dessa svårbehandlade cancerformer eftersom man då har möjlighet att nå även spridda tumörer. Detta gäller särskilt de målsökande radioaktiva läkemedlen som utnyttjar egenskaper hos tumörerna. Ett sådant exempel är behandling av neuroendokrina tumörer med ^{177}Lu-oktreotat. Neuroendokrina tumörer växer långsamt med vanligtvis vaga symtom vilket gör att de oftast upptäcks sent i sjukdomsförloppet när de hunnit sprida sig i kroppen. Cancercellerna i neuroendokrina tumörer har receptorer för hormonet somatostatin på sin cellyta. Genom att binda radionukliden ^{177}Lu till oktreotat, som är en syntetisk molekyl som binder till somatostatinreceptorer, kan ^{177}Lu på ett målsökande sätt levereras till tumörerna och bestråla dem inifrån.

Som för all cancerbehandling är målet med ^{177}Lu-oktreotat-behandling att oskadliggöra cancerceller men samtidigt skona de friska cellerna. Därför begränsas hur mycket ^{177}Lu-oktreotat som kan ges av risk för biverkningar i strålkänsliga organ, i detta fall njurarna, men även benmärg. Dagens ^{177}Lu-oktreotat-behandling resulterar oftast i förlängt liv och ökad livskvalitet, men sällan till fullständigt tillfrisknande. Bättre strålskydd av njurar och benmärg skulle möjliggöra att en större mängd ^{177}Lu-oktreotat kan ges, vilket skulle innebära bättre möjlighet att bota patienter med neuroendokrina tumörer. Antioxidanter har förmåga att minska strålningsinducerad skada på celler.

I denna avhandling presenteras resultat från studier på ifall antioxidanten α_1-mikroglobulin (A1M) skulle kunna minska effekterna från bestrålning i njurar och benmärg om den ges tillsammans med ^{177}Lu-oktreotat. För att säkerställa att A1M inte också skyddar tumörerna från strålningen från

^{177}Lu studeras även effekter i tumörvävnad. Resultaten visar att A1M inte har någon negativ effekt på behandling av neuroendokrina tumörer med ^{177}Lu-octreotate. Inget tydligt skydd mot strålningen i njurar och benmärg kunde heller visas när ^{177}Lu-octreotate gavs tillsammans med A1M.

För att optimera behandling med ^{177}Lu-oktreotat individuellt för varje patient behövs även metoder för att tidigt kunna bedöma risk för sen njurskada. Detta är särskilt viktigt då studier har visat stora skillnader i stråldos till njurarna och olika strålkänslighet mellan patienter. Genom att tidigt få indikationer på att en njurskada håller på att utvecklas kan skyddande åtgärder sättas in i tid, men kunskapen kan också användas för att identifiera vilka patienter som på ett säkert sätt kan ges en högre dos av ^{177}Lu-oktreotat. På detta sätt kan behandlingen anpassas till varje patient individuellt. Tidigare forskning har föreslagit ett flertal lovande biologiska markörer, och i detta projekt utvärderas om några av dessa kan användas för att förutse strålningsinducerad njurskada efter ^{177}Lu-oktreotat-behandling. Lovande resultat observerades för proteinet RBP4 (mätt i urin) samt proteinerna KIM-1, CDKN1A och S100A6 vars uttryck i njuren ökande med given mängd ^{177}Lu-oktreotat.

List of papers

This thesis is based on the following studies, referred to in the text by their Roman numerals.

I. Andersson C., Shubbar E., Schüler E., Åkerström B., Gram M. and Forssell-Aronsson E.
Recombinant α_1-Microglobulin Is a Potential Kidney Protector in ^{177} Lu-Octreotate Treatment of Neuroendocrine Tumors.
Journal of Nuclear Medicine, 2019;60:1600-1604

II. Rassol N., Andersson C., Pettersson D., Al-awar A., Shubbar E., Åkerström B., Gram M., Helou K. and Forssell-Aronsson E.
Co-administration with A1M does not influence apoptotic response of ^{177}Lu-octreotate in GOT1 neuroendocrine tumors. (Submitted)

III. Andersson C., Shubbar E., Parris T., Langen B., Larsson M., Schüler E., Olsson BM., Strand SE., Åkerström B., Gram M., Helou K. and Forssell-Aronsson E.
Effects of recombinant α_1-microglobulin on the early proteomic response in risk organs after exposure to ^{177}Lu-octreotate.
(Manuscript)

IV. Andersson C., Simonsson K., Shubbar E., Gram M., Helou K. and Forssell-Aronsson E.
Early apoptotic response in kidney after ^{177}Lu-octreotate administration with or without potential radioprotector α_1-microglobulin. (Manuscript)

V. Andersson C., Pettersson D., Shubbar E., Gram M., Helou K., Johansson M. and Forssell-Aronsson E.
Assessment of potential nephrotoxicity biomarkers after ^{177}Lu-octreotate administration and effects of antioxidant α_1-microglobulin.
(Manuscript)

Selection of related presentations

1. **Andersson C.**, Shubbar E., Paris T., Langen B., Larsson M., Schüler E., Olsson BM., Strand SE., Åkerström B., Gram M., Helou K., Forssell-Aronsson E. Early response in radiation related proteins in mouse kidney after injection of ^{177}Lu-octreotate with or without recombinant α_1-microglobulin. The planning group for Oncological radionuclide therapy (supported by The Swedish Cancer Society), Digital meeting, Stockholm, Sweden, 2021, June 8-10 (oral presentation)

2. **Andersson C.**, Shubbar E., Åkerström B., Gram M., Forssell- Aronsson E. rA1M, a kidney protector during PRRT? European Radiation Protection Week, Stockholm, Sweden, 2019, 14-18 October (poster presentation)

3. **Andersson C.**, Shubbar E., Åkerström B., Gram M., Forssell- Aronsson E. A1M is a potential kidney protector in ^{177}Lu-octreotate treatment of neuroendocrine tumours. 2nd European Congress of Medical Physics, Copenhagen, Denmark, 2018, August 23-25 (oral presentation)

4. **Andersson C.**, Shubbar E., Åkerström B., Gram M., Forssell- Aronsson E. Potential protection of renal function in ^{177}Lu-octreotate treatment using alpha-1-microglobulin. The European Association of Nuclear Medicine, Düsseldorf, Germany, 2018, October 13-17 (poster presentation)

5. **Andersson C.**, Shubbar E., Åkerström B., Gram M., Forssell- Aronsson E. Co-administration of rA1M during ^{177}Lu-octreotate treatment does not interfere with the therapeutic effect. The North American Neuroendocrine Tumor Society, Seattle, USA, 2018, October 4-6 (poster presentation)

Content

Abstract i

Sammanfattning iii

List of papers v

Selection of related presentations vi

Abbreviations x

1. Background **1**

1.1 Radionuclide therapy for patients with neuroendocrine tumours 1

1.2 Acute and late side effects of ^{177}Lu-octreotate 2

1.2.1 Bone marrow toxicity 2

1.2.2 Nephrotoxicity 3

1.3 Strategies for kidney protection 5

1.4 Biological responses to radiation 5

1.4.1 Classical radiobiological paradigm 5

1.4.2 Non-targeted effects 6

1.4.3 Oxidative stress 6

1.4.4 Cell death mechanisms 6

1.4.5 Apoptosis 7

1.4.6 Epigenetics 8

1.5 Radiobiology in radionuclide therapy 9

1.6 Molecular biology 9

1.6.1 From gene to protein 9

1.6.2 Methods for gene regulation analyses 9

1.6.3 Methods for protein regulation analyses 10
1.7 Radioprotectors 11
1.8 Antioxidants in cancer radiotherapy 11
1.9 α_1-microglobulin (A1M) 11
1.9.1 Structure and molecular properties 12
1.9.2 A1M as radioprotector 13
1.10 Biomarkers for kidney damage 13
2. Aims 17
3. Methods and materials 19
3.1 Radiopharmaceutical (Papers I-V) 19
3.2 Recombinant α_1-microglobulin (Papers I-V) 19
3.3 Animal experiments (Papers I-V) 19
3.3.1 Animal models (Papers I-V) 20
3.3.2 Biodistribution in GOT2 bearing mice (Paper I) 21
3.3.3 Therapeutic effects in GOT1 tumour bearing mice (Papers I-II) 21
3.3.4 Early effects on kidney and bone marrow (Papers III-IV) 22
3.3.5 Late effects on kidney tissues and urinary biomarker levels (Paper V) 22
3.4 Radioactivity measurements (Papers I-V) 22
3.4.1 Absorbed dose calculation (Papers II - IV) 23
3.5 Gene expression analyses (Papers II and IV) 24
3.6 Proteomic analyses (Paper III) 25
3.7 ELISA (Paper V) 26
3.8 Histopathological and immunohistochemical analyses (Paper V) 26
4. Results and discussions 27
4.1 Impact of A1M on the therapeutic effects of ^{177}Lu-octreotate in tumours (Papers I-II) 27
4.1.1 Biodistribution of ^{177}Lu (Paper I) 27

4.1.2 Tumour volume reduction and re-growth (Paper I) 27
4.1.3 Regulation of apoptosis related genes in tumour tissue (Paper II) 28
4.2 Early effects in kidney and bone marrow tissue (Papers III-IV) 30
4.2.1 Effects of ^{177}Lu-octreotate (Papers III-V) 30
4.2.2 Effects of A1M (Papers III-V) 32
4.2.3 Effects of ^{177}Lu-octreotate combined with A1M (Papers III-V) 33
4.3 Long-term effects in (Paper V) 37
4.3.1 Morphological signs of kidney injury (Paper V) 37
4.3.2 Biomarkers for kidney damage (Paper V) 38
5. Conclusions **41**
6. Future perspectives **43**
Acknowledgements **45**
References **47**

Abbreviations

^{111}In	Indium-111
^{131}I	Iodine-131
^{177}Lu	Lutetium-177
^{90}Y	Yttrium-90
A1M	α_1-microglobulin
ATP	Adenosine triphosphate
Bq	Becquerel
cDNA	Complementary DNA
Da	Dalton
DNA	Deoxy ribonucleic acid
EBRT	External beam radiotherapy
ELISA	Enzyme linked immunosobent assay
GFR	Glomerulus filtration rate
GO	Gene ontology
Gy	Gray
H&E	Haematoxylin and eosin
IHC	Immunohistochemistry
IPA	Ingenuity pathway analysis
i.v.	Intravenous
keV	Kilo electron volt
LC-MS/MS	Liquid chromatography mass spectrometry
MIRD	Medical Internal Radiation Dose Committee
MOMP	Mitochondrial outer membrane permeabilization
mRNA	messenger RNA
NaCl	Sodium chloride
NET	Neuroendocrine tumour
PBS	Phosphate buffered saline solution
PCR	Polymerase Chain Reaction
PRIDE	Proteomic identifications database
RIN	RNA Integrity Number
RNA	Ribonucleic acid
RT-qPCR	Quantitative reverse transcription PCR
SSTR	Somatostatin receptor
tRNA	Transfer-RNA

1. Background

1.1 Radionuclide therapy for patients with neuroendocrine tumours

Still, after many years of research, the majority of patients with malignant disseminated cancer are difficult to cure. Radiopharmaceuticals have proven to be useful for treatment of tumour metastases, since they have the potential to target disseminated tumour cells. During the last decades, improvement in the tumour-specificity of radionuclide therapy have been achieved by developing radiopharmaceuticals that utilises certain properties of the tumours. Radiolabelled somatostatin analogues, used for treatment of neuroendocrine tumours (NETs), is one example.

Many NETs display high levels of membrane bound somatostatin receptors (SSTRs), while most other normal tissues express low levels of SSTRs. By attaching a radionuclide to a somatostatin analogue and administering this compound systemically to the patient, higher uptake of the radionuclide in the tumours compared with normal tissues will then be achieved [1, 2]. Initial attempts were made with ^{111}In-octreotide using the emission of Auger and conversion electrons from ^{111}In [3-6]. The therapeutic effects were modest, mainly since ^{111}In is less suitable for therapy due to the high energy emitted as photons [7]. Octreotide labelled with the β emitter ^{131}I to tyrosine was also studied, but a fast degradation was observed (biological half-life less than 1 hour) and ^{131}I-Tyr-octreotide was therefore found to be less suitable for targeted radionuclide therapy [8]. More recent clinical studies with the β emitters ^{90}Y (emitting electrons with an average energy of 0.933 MeV per nuclear transformation [9] or ^{177}Lu (emitting electrons with an average energy of 0.148 MeV per nuclear transformation [9]) attached to DOTA-octreotate have shown promising therapeutic effects, although mild side effects on bone marrow and kidneys have been reported [10-13]. Comparative studies on ^{90}Y-octreotide and ^{177}Lu-octreotate have concluded that ^{177}Lu-octreotate have a more favourable toxicity profile, most probably due to the shorter range of the emitted electrons from ^{177}Lu compared to ^{90}Y electrons [14, 15].

In October 2017, based on the promising results from the NETTER-1 randomized phase III clinical trial [16], ^{177}Lu-octreotate was approved by the European Medicines Agency (EMA) and then later by the United States Food and Drug Administration (FDA) in 2018. ^{177}Lu-octreotate (Lutathera®, Advanced Accelerator Applications) is market authorised for treatment of inoperable, metastatic or progressive, well differentiated SSTR positive gastroenteropancreatic NETs in adults [17]. The approved treatment protocol consists of up to 4 fractions of 7.4 GBq given with intervals of 8-16 weeks [18]. Although the clinical results so far are promising, with clearly prolonged patient survival, they are still modest compared with the cure rate seen *in vivo* in animal NET models. Furthermore, clinical trials preceding NETTER-1 also demonstrated that most patients will tolerate higher number of fractions [19-21]. Hence, there is a need for optimisation of ^{177}Lu-octreotate treatment [22]. A more aggressive treatment with higher administered activity or more fractions would allow for better tumour control and higher cure rate. However, side effects on normal tissues will limit the administered activity that can be given to the patient, where bone marrow and the kidneys are the main dose limiting organs [21, 23-25].

1.2 Acute and late side effects of ^{177}Lu-octreotate

Acute side effects from treatment with ^{177}Lu-octreotate are in general mild and easy to manage. Nausea is a common acute side effect, as well as vomiting, abdominal pain, mild hair loss and mild asthenia [10, 19]. Mild effects on the bone marrow has also been reported as an acute side effect [19]. Reports of late side effects includes a few cases of kidney and liver toxicity [10].

1.2.1 Bone marrow toxicity

In systemic radionuclide therapy the bone marrow is irradiated by the circulating activity in the blood, but is also taking up radiolabelled somatostatin analogues [1]. The bone marrow is due to its rapidly dividing hematopoietic stem cells (cells that develops into other blood cells) a radiosensitive and early responding organ. A commonly used dose limit for the bone marrow is 2 Gy in total. The bone marrow status is monitored by blood analyses of haemoglobin concentration, white blood cell counts and platelet counts. Radiation induced bone marrow toxicity is kept low by having intervals of ca 8-16 weeks between the fractions (administrations of ^{177}Lu-octreotate) [18], which allows the bone marrow to

recover. Effects on the bone marrow may still be observed after the treatment, although in most cases full haematological recovery is achieved [19].

1.2.2 Nephrotoxicity

One of the main functions of the kidneys is to filter blood from waste products and to excrete them via the urine. The glomerulus, proximal tubule, loop of Henle, distal tubule and the collecting duct are the main parts of the kidneys functional unit, the nephron, see Figure 1.1 The kidney can be divided into two parts, cortex and medulla. The cortex is the outer part of the kidney and (somewhat simplified) includes the glomerulus, proximal tubules and distal tubule. The medulla is the inner part of the kidneys where the major parts of the loop of Henle and the collecting ducts are found, but also contains glomeruli and tubules. The medulla can further be divided into an inner and an outer part.

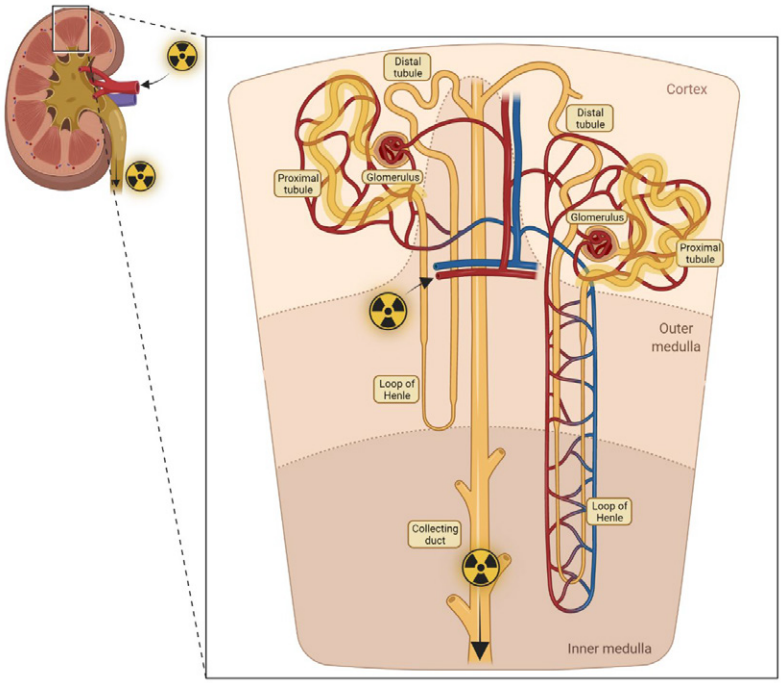

Figure 1.1 Renal handling and retention of ^{177}Lu-octreotate. Schematic image of the nephron illustrating filtration and retention of ^{177}Lu after systemic administration of ^{177}Lu-octreotate. The radiopharmaceutical is filtered in glomerulus, partly reabsorbed from the primary urine and retained in proximal tubule. Un-reabsorbed ^{177}Lu leaves the body via the urine. Illustration is created with BioRender.com.

After administration of ^{177}Lu-octreotate, the majority of the ^{177}Lu activity will be filtered in the glomerulus and most of the activity will leave the body through the urine. Although, a small portion of the injected activity will be retained in the kidney tissue due to reabsorption in proximal tubules and collection ducts [26]. The reabsorption/retention processes are not fully understood, but it is known to at least partly occur via protein receptors such as the megalin-cubilin complex. The positively charges somatostatin analogues have been found to bind to the negatively charged megalin-cubilin complex [26]. Indications of internalisation of radiolabelled somatostatin analogues by endocytosis followed by transported to lysosomes in the proximal tubule cell have been observed. Due to the high expression of megalin-cubilin, the complex is considered to be the main source of ^{177}Lu uptake in proximal tubules [13, 26]. Another potential cause of retention of ^{177}Lu-octreotate is SSTRs. There are five subtypes of SSTR and octreotate have the highest affinity to subtype 2 [27]. In man and mice, all five subtypes of SSTR are expressed in the kidney [28-31]. The expression of SSTR2 has been observed at several locations in human and mouse nephrons; in glomerulus, proximal and distal tubules, loop of Henle, and in the collecting ducts. In rat, the SSTR2 expression is limited to glomerulus and collecting ducts [28]. At present, it is still not known how much the SSTR expression contributes to the renal retention of ^{177}Lu.

The distribution of radiolabelled somatostatin analogues in the kidneys following injection has been found to be heterogeneous [26, 32]. Highest accumulation of ^{177}Lu, following ^{177}Lu-octreotate injection, has been found in cortex in rat kidney. Similar heterogeneous distribution was found in mice and rat for ^{111}In following injection of ^{111}In-octreotide or ^{111}In-octreotate. In another study, comparing the kidney distribution of ^{111}In-octreotide in male and female rats and mice, differences between ^{111}In activity in renal cortex and renal medulla were observed [33]. In rats, the highest uptake of ^{111}In-octreotide was observed in cortex with less activity in outer medulla; 24 h after injection the ratio between activity concentration in cortex (C) and outer medulla (OM) (C/OM) was about a factor of 3 for both female and male rats. In male mice, the highest uptake was also found in the cortex, while female mice had less ^{111}In in cortex and highest ^{111}In concentration was found in outer medulla, with a C/OM of 0.7 compared with 1.2 in male mice. In humans, the ^{111}In activity following ^{111}In-octreotide injection was found to be mainly, but not exclusively, localized in cortex [34].

1.3 Strategies for kidney protection

Proposed strategies to overcome the risk of kidney toxicity in SSTR based radionuclide therapy, is well summaries by Geenen. L *et al* and Forssell-Aronsson E *et al* [22, 25]. In short, there are three main approaches to improve kidney protection:

1) modifying the characteristics of the radiopharmaceutical
2) reduce the uptake in the kidneys
3) reduce the radiobiological effects in the kidneys

Radioprotective measures that are used today include chose of radionuclide (choosing ^{177}Lu over ^{90}Y), and co-infusion of kidney blocking agents, usually lysine and arginine. These blocking agents are positively charged amino acids that only partly block the uptake and retention of the radio-peptide in the kidneys and can cause nausea and vomiting [35, 36].

Although efforts are made to protect the kidneys, the tumour treatment is still limited by the potential risk of late kidney toxicity. Hence, there is a need for new adequate methods that can ensure protection of normal tissue in order to allow a more effective treatment. The first and the second approaches to improve kidney protection goes hand in hand and aims to reduce the radiation exposure of the kidney. This thesis is focussed on improving the protection of the kidney using the third approached: to reduce the radiobiological effects in kidney tissue.

1.4 Biological responses to radiation

1.4.1 Classical radiobiological paradigm

According to the classical radiobiological paradigm, ionizing radiation can damage the tissue either by direct interaction with the target or by indirect interaction with the target via interaction with surroundings and release of free radicals that then interact with the target. The primary affected cell compartments are DNA, but also mitochondria and the cell membrane may act as targets. The overall cellular response to irradiation is to 1) recover (successful repair), 2) induce DNA mutations resulting in accumulation of genetic alterations and potential cancer initiation and development (non-successful repair), or 3) die. [37-40]

1.4.2 Non-targeted effects

It has been shown that radiation induced effects are not limited to the irradiated cell. Irradiated cells can induce effects in non-irradiated neighbouring cells (bystander effect) or even distant cells in other organs or parts of the body (abscopal effects). These and other effects are referred to as non-targeted effects that cannot be explained by the classical radiobiological paradigm. These types of effects include cell-cell signalling mediated by gap junctions and inflammatory related molecules. [39-42]

1.4.3 Oxidative stress

Radiolysis of water is initiated in tissue when exposed to ionizing radiation. This process produces, e.g., reactive oxygen species (ROS) and reactive nitrogen species (RNS) which can cause a toxic condition in the tissue known as oxidative stress. ROS/RNS are counteracted by endogenous antioxidants defence mechanisms and oxidative stress is caused when there is an imbalance between pro- and antioxidants. Radiation induced oxidative stress can cause damage to proteins, lipids, and DNA in irradiated cells, but can also effect neighbouring cells. Reduction and oxidation (redox) reactions are initiated short time after irradiation and play an important role in the early radiobiological response. Redox processes can cause acute radiation damage, but has also been found to cause late effects like chronic inflammation.[43]

1.4.4 Cell death mechanisms

Radiation has been found to induce several types of cell death mechanisms including but not limited to apoptosis, autophagic cell death, necroptosis, necrosis, mitotic catastrophe and cellular senescence. Which types of cell death that are initiates is dependent on radiation related factors such as dose, dose-rate and type of radiation, but also on biological factors like oxygen level, cell cycle phase, p53 mutation status, and the capacity to repair DNA. Differences in radiation induced cell death mechanisms is observed between malignant tissue and normal tissues, which can be utilized to enhance radiosensitivity in tumour tissue or enhance radioresistance in normal tissues. [44]

In this thesis work the focus is on radiation induced apoptosis, which is described in more detail in the section below.

1.4.5 Apoptosis

Apoptosis is a form of regulated (programmed) cell death that often is described as one of the main cell death mechanisms following radiation exposure [45]. There are two main apoptotic pathways, intrinsic and extrinsic pathways that both can be activated by radiation. The main steps are illustrated in Fig. 1.2.

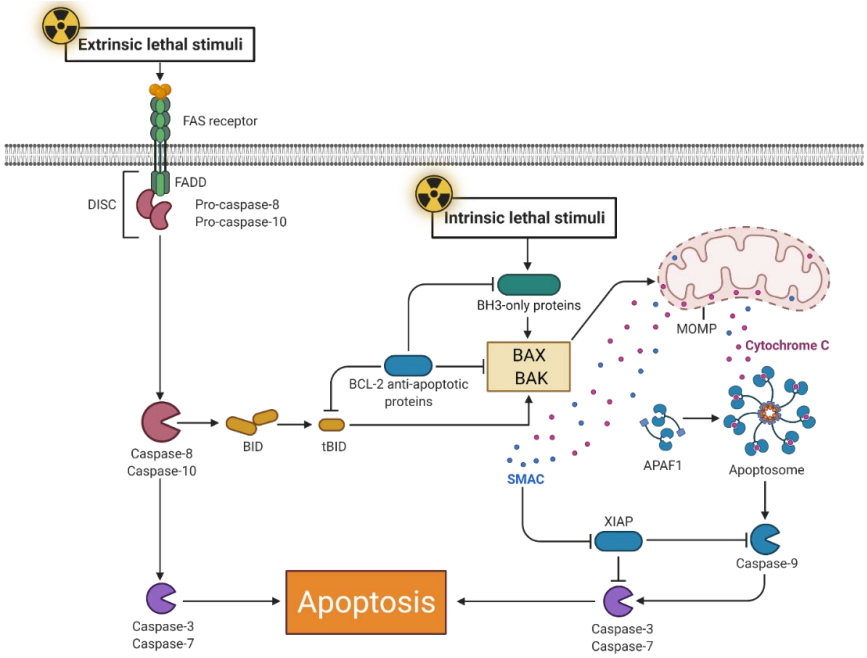

Figure 1.2 Apoptosis signalling simplified. The main steps of extrinsic and intrinsic pathway to apoptosis. See text for details. Illustration is adapted from "Apoptosis Extrinsic and Intrinsic Pathways", by BioRender.com (2022). Retrieved from https://app.biorender.com/biorender-templates

A critical event in both apoptosis pathways is mitochondrial outer membrane permeabilization (MOMP). MOMP is regulated by a complex network of interactions of pro- and anti-apoptotic proteins belonging to the B cell CLL/lymphoma-2 (BCL-2) family. Effector proteins BCL2-associated X protein (BAX) and Bcl-2 homologous antagonist/killer (BAK) are pro-apoptotic proteins, known as the effector or BAX like proteins of the BCL-2 family. Upon activation, BAX/BAK forms pores in the mitochondrial membrane, initiating MOMP and release mitochondrial proteins, like cytochrome c and second mitochondrial activator of caspases (SMAC). Once cytochrome c is released into the cytosol it will form a protein complex, known as apoptosome, by binding to apoptotic

protease-activating factor 1 (APAF1). The formation of apoptosome will result in activation of initiator caspase 9 which in turn activates the effector caspases 3 and 7, executing the final steps to apoptosis. Counteracting this process is the anti-apoptotic protein X-linked inhibitor of apoptosis (XIAP), which binds to and blocks the caspases from driving the pro-apoptosis signaling further. XIAP is in turn inhibited by cytosolic SMAC. MOMP has been described as point-of-no-return, although if only a limited number of mitochondria in the cells experience MOMP, the cell may survive. [46]

The intrinsic pathway is initiated by intrinsic lethal stimuli such as DNA damage, hypoxia and oxidative stress. In the intrinsic apoptosis pathway, BAX and BAK are activated directly or indirectly by the BH3-only proteins in the BCL-2 family. This process is balanced by the BCL-2 anti-apoptotic genes that act as inhibitors to the BH3-only proteins and also to BAX/BAK. The extrinsic apoptosis pathway is on the other hand mainly initiated by plasma-membrane receptors from the TNF receptor superfamily: tumor necrosis factor receptor superfamily member 6 (FAS) and tumor necrosis factor receptor superfamily member 10B (TNFRSF10B). These death receptors are activated by extrinsic lethal stimuli that recruit Fas associated via death domain (FADD) and pro-caspase 8 and 10, assembling the death-inducing signaling complex (DISC). Pro-caspase 8 and 10 are then transformed into its active forms caspase 8 and 10 and are released from DISC. Here the extrinsic apoptosis pathway is divided into two: 1) activation of caspase 3 and 7 or 2) cleavage of BID into tBID leading to activation of BAX/BAK and taking the route to apoptosis via MOMP. [46]

1.4.6 Epigenetics

Epigenetic effects are effects that causes changes in gene expression without causing alterations in the DNA sequence itself. DNA methylation, miRNA (non-coding RNA) and histone modifications are examples of epigenetic mechanisms that have been observed in tissue in response to radiation. There is still much that is unknown about radiation induced epigenetic effects. In recent years, the importance of epigenetic mechanisms in development of damage in irradiated tissue has become more prominent. [43]

1.5 Radiobiology in radionuclide therapy

The biological effects of ionizing radiation in tissue is complex and there are still missing pieces of the puzzle that can be useful for optimization of radionuclide therapy. Whether the intention is to increased tumour control or improve radiation protection of risk organs, a good understanding of the radiobiology of the therapy is needed [47-49]. Profiling radiation induced regulation of proteins and genes are powerful tools to get a better understanding of radiation induced effects and to identify biomarkers for radiation damage [50, 51].

1.6 Molecular biology

1.6.1 From gene to protein

Proteins have multiple functions in the body, and besides being building material, they are also hormones, enzymes, receptors, antibodies etc. Upon stimuli, (e.g. DNA-damage or growth factors) cells respond by synthetizing specific proteins. The DNA located in the cell nucleus is the template of each single protein. Simply put, a DNA sequence that codes for a protein is called a gene. One gene can code for several proteins and there are also non protein coding genes. A single-stranded copy of the gene is synthetized through transcription and further spliced into messenger RNA (mRNA) or transcript and is transported to the ribosomes in the cytoplasm where the protein synthesis takes place. Ribosomes use the mRNA as instruction template to assemble the protein, a process known as translation.

1.6.2 Methods for gene regulation analyses

The transcriptome is the complete setup of all transcripts expressed by an organism/tissue/cell at a certain time-point. Gene expression profiles can be analysed by RNA expression microarray and RNA sequencing. Quantitative real time polymerase chain reaction (qPCR) is a sensitive and well established method to analyse expression of one or several predetermined genes. The basic principle of qPCR is amplification and quantification of a DNA-sequence during repeated cycles. Prior to the assay, RNA in the sample is reversely transcribed to complementary DNA (cDNA). The double stranded cDNA is denaturised into single strands by heating. Primers, designed to bind to the specific DNA-sequence (gene) of interest, are used to identify starting point of elongation. DNA

polymerase builds complementary strand to single-stranded cDNA, creating copies of the DNA-sequence. During the process of synthesis, primers bind to the DNA-sequence copies and emit a fluorescent signal proportional to the amount of PCR product. The fluorescent light is measured at the end of each cycle and the amplification cure (intensity *vs* cycle number) is used to calculate the starting amount of the DNA-sequence in the sample.

1.6.3 Methods for protein regulation analyses

Methods to detect a specific protein are often antibody based using antibodies that are designed to identify and attach to a specific antigen, the protein of interest. Probes that bind to the antibody are used to make the antibody-antigen complex detectable, e.g. by fluorescent light or change of colour. Western blot and enzyme-linked immunosorbent assay (ELISA) are methods for determining protein concentration in cells, tissues, urine or blood. In Western blot, the proteins are first separated by molecular weight using gel electrophoresis, creating a ladder of protein bands, followed by hybridization with different antibodies and visualized by chemiluminescence or fluorescent light. In ELISA, the sample and antibody cocktail are added to pre-coated wells. The probe changes the optical density of the solution and the light absorption is proportional to the amount of the protein present in the sample. Immunohistochemistry (IHC) is a well-established method used to visualize the protein concentration and cellular localization using sections from tissues embedded in paraffin. The sections are also commonly used to study the histology of tissue, using haematoxylin (staining cell nuclei purplish) and eosin (staining cytoplasm and extracellular matrix pinkish).

Proteome wide analysis methods allow the investigation of all expressed proteins in an organism/tissue/cell at a certain time-point. Liquid chromatography mass spectrometry (LC-MS/MS), with a bottom up approach is commonly used in proteomics. In brief, proteins are first digested into peptides, separated by mass to charge and then further split into peptide fragments. Identification of the original proteins are performed by matching experimental mass spectrum of the peptide fragments (known as the MS/MS spectra) to theoretical fragmentation spectra from a database.

1.7 Radioprotectors

Radioprotectors and radiomitigators can be used to either prevent the cells from being damaged or by facilitating the recovery of the irradiated tissue. There are many approaches that can be applied to achieve radiation protection, including reduction of the level of free radicals, enhancement of DNA repair and inhibition of apoptosis. Radical scavenging is one of the main actions of antioxidants, which makes them potentially useful as radioprotectors [38].

1.8 Antioxidants in cancer radiotherapy

Antioxidants in radiation therapy of cancer is a complex topic, filled with conflicting results [52-55]. Beside their potential use in radioprotection of risk organs, antioxidants have also been suggested to protect against cancer. On the other hand, there are studies showing that antioxidants can increase progression of already existing cancer [56, 57]. The controversial results seem to be a consequence of the actual antioxidant, cancer type and framework and experimental design of the studies. There are many factors that needs to be considered, and there is no general answer to the question if supplements of antioxidants in cancer treatment is efficient and safe [58]. When introducing an antioxidant to be combined with radiotherapy in order to reduce side effects, it is therefore important to consider the potential influence the antioxidant may have on the tumour tissue. Questions that needs to be raised are:

1) does the radiation protective ability of the antioxidant also protect the tumour cells?

2) does supplement with the antioxidant benefit tumour growth or increase metastiation?

1.9 α_1-microglobulin (A1M)

In this thesis work, the potential use of a recombinant form of the endogenous antioxidant α_1-microglobulin (A1M) as kidney protector during treatment with ^{177}Lu-octreoate was investigated.

1.9.1 Structure and molecular properties

A1M has been described as a “radical sink” and “tissue housekeeping protein”, protecting tissues from oxidative stress [59, 60]. Intravascular, A1M has been shown to bind and degrade heme and to stabilize and protect red blood cells from hemolysis (rupturing of red blood cells) [61, 62]. Extravascular A1M is suggested to protect and repair the extracellular matrix and to counteract lipid peroxidation of cell membranes caused by free radicals [63, 64]. When internalized by the cells, A1M have shown to possess mitochondria protective properties, reducing oxidative stress and contribute to maintained mitochondrial homeostasis and ATP-production [65]. [66]

A1M has a relative constant serum concentration of 1-2 μM and is found in the extravascular space in most organs [67]. The liver is the primary site of production and after circulation A1M is filtered in glomerulus in the kidneys and degraded in the proximal tubules [68, 69]. It is a small glycoprotein (26 kDa) and a member of the lipocalin family. It has a structure of an eight-stranded β-barrel, a bucket like shape with closed bottom and open top, see Fig 1.3. The inside of the “bucket” is a binding site for small hydrophobic molecules. Important side-chains (highlighted in Fig 3) include Cys34 (important for radical scavenging and heme binding), Lys side-chains (involved in reductase activity) and Tyr22 and Tyr132 (involved in radical scavenging).[66, 70]

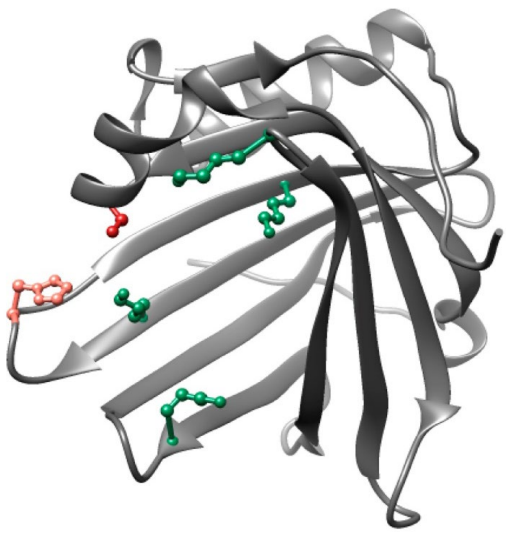

Figure 1.3 Illustration of the molecular structure of A1M. Important side-chains in the A1M structure are highlighted: Cys34 (red), His123 (pink), Lys69 (green), Lys92 (green), Lys118 (green) and Lys130 (green). Reprint from [71], with kind permission from Amanda Kristiansson.

1.9.2 A1M as radioprotector

A1M has shown to inhibit the propagation of radiation induced cell death in bystander cells [64, 72] and has previously been proposed as radioprotector during ^{177}Lu-octreotate treatment [70, 71]. It is the radical scavenging properties and its distribution in the kidneys upon infusion (co-localization with ^{111}In-octreotide) that are the main arguments for A1M as a kidney protector. Its potential kidney protecting abilities during ^{177}Lu-octreotate treatment have so far only been investigated in one study [73]. The results showed less radiation induced renal damage in mice when ^{177}Lu-octreotate was combined with A1M. This was indicated by better overall survival, less DNA damage (measured by γH2AX foci) and better preserved morphology (determined by histological evaluation) in the kidneys from mice in combination group. In the same study, the regulation of genes related to apoptosis were investigated in the kidney. At 24 hours after injection a clear difference in response between the groups was observed with almost no regulation in the apoptotic genes in the combination group, while regulation was found in almost all apoptotic genes studied in the ^{177}Lu-octreotate group. In a later study, kidney function was investigated in mice co-infused with A1M and ^{177}Lu-PSMA-617 (used to treat prostate cancer) [74]. The results showed somewhat preserved renal function in mice receiving A1M following ^{177}Lu-PSMA-617 injection compared with the mice receiving ^{177}Lu-PSMA-617 without A1M.

In summary, *in vitro* and *in vivo* results indicate promising prospects of A1M as a kidney protector during ^{177}Lu-octreotate treatment. However, the mechanisms behind kidney protection by A1M is not fully understood and needs be further investigated both for A1M alone and in combination with radiation.

1.10 Biomarkers for kidney damage

Methods for detection of reduction of kidney function during ^{177}Lu-octreotate treatment include the use of specific biomarkers. A biomarker is “a measurable indication of a specific biological state that is relevant for a specific process” [75]. An ideal biomarker is originated from the damaged cells and is specific for the organ of interest, and at the best is detectable in blood or urine. It should also have a direct correlation to the degree of damage.

The most common method for kidneys function estimation is monitoring of glomerulus filtration rate (GFR), e.g. by measuring changes in serum creatinine

or serum and urinary cystatin C levels [76, 77]. Creatinine is a rest product from muscle metabolism and is excreted to the urine via glomerulus filtration, without reabsorption in the tubules. The production of creatinine is relative constant and increase of serum creatinine (or reduction in urinary creatinine) indicate damage to glomerulus. Creatinine is however greatly influenced by non-renal related factors such as muscle mass, age and gender [78], which makes it less optimal as biomarker. Cystatin C is produced in all nucleated cells and filtered in the kidneys. Unlike creatinine the major part of cystatin C is reabsorbed from the primary urine and degraded in proximal tubules [79]. Evaluated levels of cystatin C in the urine can be an indication of damaged proximal tubules. Cystatin C is not as influenced by muscle mass, age and gender as creatinine and may be a more robust alternative to creatinine [79]. However, cystatin C has other confounders, such as thyroid function and inflammation that need to be considered [77]. Other methods to estimate kidney function are ^{99m}Tc-DTPA, -DMSA and -MAG3 scintigraphy. ^{99m}Tc-DTPA is used to estimate GFR; the uptake and clearance of ^{99m}Tc-DTPA from plasma is directly related to GFR with no contribution from secretion or reabsorption [80]. ^{99m}Tc-DMSA and -MAG3 are used for imaging dysfunctional or non-functional regions of the kidney, and MAG3 is excreted from the blood via the proximal tubules [81, 82].

Radiation induced kidney damage from ^{177}Lu-octreotate treatment is complex, usually occur late after exposure and may include damage to both glomerulus and tubules. This might explain why GFR (estimated with serum creatinine) has shown to be a poor biomarker for ^{177}Lu-octreotate induced renal dysfunction [19]. Furthermore, the methods that are used in the clinic today are thus limited to late evaluation of effects in the kidney after radiation exposure. In order to improve kidney protection in radionuclide therapy and to get a more effective prevention of functional loss, early detection of renal impairment is preferred.

Several protein biomarkers have been proposed as early indicators of kidney damage, e.g., neutrophil gelatinase-associated lipocalin (NGAL), kidney injury molecule-1 (KIM-1) and retinol binding protein 4 (RBP4) [82-84]. NGAL is one of the most widely studied biomarker of acute kidney damage and is a marker for tubular inflammation. The primary site of NGAL production is loop of Henle and collecting ducts in the kidneys. Under normal conditions the kidney expression is low, but upon injury, NGAL is rapidly upregulated and secreted from the kidney. NGAL is then filtered in glomerulus with reabsorption in the proximal tubules resulting in increase of urinary NGAL, further elevated by potential damage to proximal tubules [83]. KIM-1 has normally a weak to moderate expression in kidney tubule epithelium and plays an important role in maintaining and repairing

the epithelium. When the renal epithelium is stressed or damaged, KIM-1 is upregulated, and elevated urinary KIM-1 is not just a marker for induced renal damage it may also indicate induced reparation processes [85]. RBP4 is mainly produced in the liver and secreted to the blood where it acts as a vitamin A transporter. Due to its small weight (21 kDa) it is freely filtered in glomerulus with more than 99% reabsorption in proximal tubules. Consequently, increased RBP4 concentration in the urine is an indicator of proximal tubules dysfunction. Urinary RBP4 has been found to be a sensitive and early indicator of damage to the proximal tubule [86]. The properties of NGAL, KIM-1 and RBP4 are more similar to the ideal biomarker than creatinine. However, it remains to be investigated if these promising biomarkers are suitable for early detection of late radiation induced kidney damage from ^{177}Lu-octreotate treatment.

In our research group, we have previously studied correlation between radiation-induced renal impairment and urinary levels of RBP4 in mice, demonstrating early increase of RBP4 excretion 30 days after injection of 60 or 120 MBq ^{177}Lu-octreotate [87]. We have also performed transcriptomic and proteomic analysis and identified several biomarkers for kidney damage induced by ^{177}Lu-octreotate in mouse models [88-91]. Prominent findings include dose-dependent regulation of the *Cdkn1a* (cyclin-dependent kinase inhibitor 1A) and *Lcn2* (NGAL) and regulation of S100 calcium binding protein A6 (*S100a6*) and adiponectin (*Adipoq*) at both early and late time points after ^{177}Lu-octreotate injection [92]. Expression of the *Havcr1* (KIM-1) gene was found to be significantly regulated at several absorbed doses at an early time-point after ^{177}Lu-octreotate injection [90]. However, regulation of *Havcr1* was rarely seen at time-points later than one week after ^{177}Lu administration [89, 92]. To evaluate the clinical significance of these biomarkers, further studies on, e.g., blood and urine samples collected after radionuclide administration are needed to establish dose-response relationship, timing and correlation with GFR reduction.

2. Aims

The overall aim of this thesis was to investigate the possibility to improve treatment of NET with ^{177}Lu-octreotate by reducing the effects in normal tissue with the use of the proposed radioprotector A1M.
Radiobiological effects in NET models were investigated *in vivo* to ensure maintained therapy effect when^{177}Lu-octreotate where co-administrated with A1M. The specific aims were to investigate:

- if co-administration of ^{177}Lu-octreotate and A1M impacts the biodistribution of ^{177}Lu in GOT2 NET bearing mice **(Paper I)**
- if co-administration of ^{177}Lu-octreotate and A1M impacts the radiation induced change in GOT1 NET volume in mice **(Paper I)**
- expression of apoptosis related genes in GOT1 NET in mice early (1 and 7 days) after administration of ^{177}Lu-octreotate with or without A1M and A1M alone **(Paper II)**

Radiobiological effects in risk organs were studied in normal mice after ^{177}Lu-octreotate administration with or without co-administration of A1M and A1M alone. The specific aims were to investigate:

- protein expression in bone marrow and kidney tissue early (1 and 7 days) after administration of ^{177}Lu-octreotate with or without A1M and A1M alone **(Paper III)**
- expression of apoptosis related genes in kidney tissue early (1 and 7 days) after administration of ^{177}Lu-octreotate with or without A1M and A1M alone **(Paper IV)**
- potential use of urinary RBP4, NGAL, creatinine and cystatin C as biomarkers for ^{177}Lu-octreotate induced kidney damage, and to compare data with corresponding results from mice co-administered with ^{177}Lu-octreotate and A1M **(Paper V)**
- expression of NGAL, KIM-1, CDKN1A, S100A6 and ADIPOQ in kidney 9 months after ^{177}Lu-octreotate exposure, to further validate these proteins as indicators of toxicity and to compare data with corresponding results from mice co-administered with ^{177}Lu-octreotate and A1M **(Paper V)**

3. Methods and materials

3.1 Radiopharmaceutical (Papers I - V)

Preparation of ^{177}Lu-octreotate was conducted according to the manufacturer's instructions. LuMark® ^{177}Lu chloride and peptide was obtained from Nuclear Research and Consultancy Group (IDB Holland). Amount of peptide bound ^{177}Lu was >97%, determined using instant thin layer chromatography.

3.2 Recombinant α_1-microglobulin (Papers I - V)

Human recombinant A1M (A1M-035 [93]) was used in all experiments (referred to as A1M or rA1M). A1M and A1M vehicle solution (containing sterile endotoxin-free 10 mM Na3PO4 (pH 7.4), 0.15 M NaCl, and 12 mM histidine) were supplied by A1M Pharma (Lund, Sweden) (new name: Guard Therapeutics International AB, Stockholm, Sweden). An A1M dose of 5.0 mg/kg (body weight) was used in all experiments, administrated by tail vein injection.

3.3 Animal experiments (Papers I - V)

An overview of the animal experiments in this thesis are illustrated in Figure 3.1

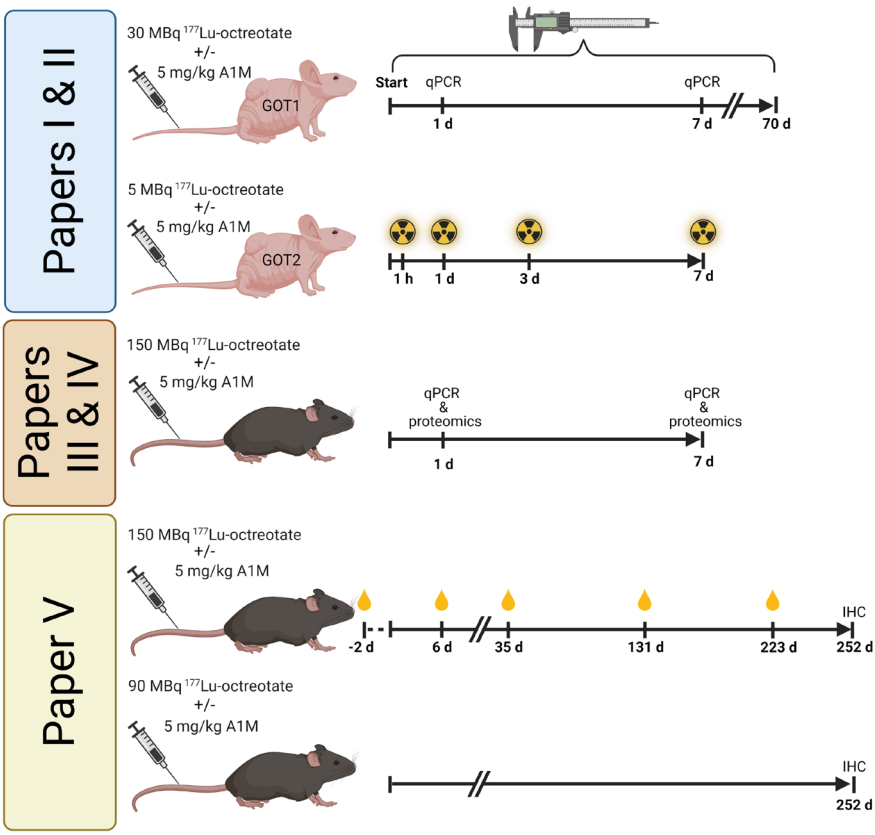

Figure 3.1 Overview of the conducted animal experiments in this thesis. Control groups were used to match the study groups viewed in the illustration. The illustration was created using BioRender.com.

3.3.1 Animal models (Papers I - V)

All animals in the studies were kept under standard laboratory conditions with free access to food and water and daily supervision. All studies were approved by the Ethics Committee for Animal Research in Gothenburg, Sweden, ID 146-2015 and 107-2015. Effects on normal tissues were studied in female C57BL/6N mice from Charles River Laboratories (Germany). Two animal tumour models were used to investigate effects on tumour tissue: GOT1 and GOT2. Both models include slowly growing human NETs with preserved neuroendocrine properties. GOT1 is a small intestine NET, originally derived from a liver metastasis from a 55-year-old female patient [94]. GOT2 is a medullary thyroid carcinoma model originally derived from a cervical lymph node metastasis from a 79- year-old male patient [95]. Pieces of the tumours were transplanted under the skin in the neck or on the

flank of female BALB/c nude mice from Janvier Labs (France) or Charles River Laboratories (Germany). The transplantations were performed according to previously published method [94, 95].

3.3.2 Biodistribution in GOT2 bearing mice (Paper I)

The biodistribution of ^{177}Lu after injection of ^{177}Lu-octreotate were investigated in GOT2 bearing mice. A low activity level of 5 MBq was chosen to avoid therapeutic effects (reduction in tumour volume) during the study time. Mice were injected in the tail vein with 5 MBq ^{177}Lu-octreotate, half of them also received A1M injection. The mice were killed in groups of 4 at 1, 24, 72 and 168 hours after injection. At the time of death samples of blood, lungs, liver, spleen, kidneys, tumour, femur (with bone marrow), adrenal glands and pancreas were collected and weighed, and ^{177}Lu activity in the samples was measured in a gamma counter, see below. Statistically significant differences between the groups were determined by two-way ANOVA (statistical significance were considered for $p>0.05$).

3.3.3 Therapeutic effects in GOT1 tumour bearing mice (Papers I- II)

A moderate activity level of 30 MBq was chosen to resemble the clinical situation with tumour reduction without complete remission. The volume of GOT1 tumours in mice injected with 30 MBq ^{177}Lu-octreotate, 30 MBq + A1M, or A1M, and in untreated control mice were followed over time. The volumes were measured using a digital slide callipers, assuming an elliptic shape of the tumours. Volume over time for each individual tumour were integrated using the trapezoidal rule and net change in tumour volume was calculated. Statistically significant differences in net change in tumour volume were determined by Kruskal-Wallis one- way ANOVA (statistical significance were considered for $p>0.05$).

Expression of apoptosis related genes was investigated in GOT1 tumours from mice injected with 30 MBq ^{177}Lu-octreotate, 30 MBq ^{177}Lu-octreotate + A1M, or A1M, and in control mice injected with phosphate buffered saline solution (PBS). Half of the number of animals were killed after 1 day and the rest after 7 days. At the time of death, samples of GOT1 tumour tissue were collected and flash frozen. Later, gene expression of apoptosis related genes were analysed in GOT1 tumour tissues.

3.3.4 Early effects on kidney and bone marrow (Papers III-IV)

Early effects of ^{177}Lu-octreotate and A1M were investigated in mouse bone marrow, kidney medulla and kidney cortex tissue. A high activity level of 150 MBq was chosen to inflict radiobiological effects that later would develop to radiation damage in the kidneys [92]. Mice were divided into five groups and injected with a) 150 MBq ^{177}Lu-octreotate and PBS, b) A1M and PBS, c) 150 MBq ^{177}Lu-octreotate and A1M, d) two times PBS, or e) PBS and A1M vehicle solution. Half of the number of mice in each group was killed at 1 day and the other half at 7 days post injection. From each mouse both femurs and one of the kidneys were flash frozen and stored at – 80°C. Separation of bone marrow from femur and dissection of frozen kidney medulla and kidney cortex were performed on dry ice using a scalpel. Proteomic analyses were conducted on frozen samples of bone marrow, kidney medulla and kidney cortex and gene expression of apoptosis related genes were analysed in the kidney medulla and kidney cortex samples.

3.3.5 Late effects on kidney tissues and urinary biomarker levels (Paper V)

Kidney function and toxicity were investigated in mice injected with 1) 90 MBq ^{177}Lu-octreotate + PBS, 2) 150 MBq ^{177}Lu-octreotate + PBS, 3) 90 MBq ^{177}Lu-octreotate + A1M, 4) 150 MBq ^{177}Lu-octreotate + A1M, 5) A1M + PBS, or 6) Two times PBS. Repeated urine samples were collected from 2 days before injections up to day 223 after injection. The urine was flash frozen and later measured for concentrations of cystatin C, NGAL and RBP4 using ELISA. The study was ended after 9 months, the animals were killed and kidneys were sampled for immunohistochemical analyses.

3.4 Radioactivity measurements (Papers I - V)

The ^{177}Lu activity in syringes was measured by a calibrated well-type ionization chamber (CRC-15R; Capintec, New Jersey, USA), and the ^{177}Lu activity in tissue samples was measured by a gamma counter (2480 Wizard 147 Automatic Gamma Counter, PerkinElmer, Waltham, USA). The measurement data from the gamma counter was corrected for background radiation and dead time losses. Both detectors were cross calibrated.

The ^{177}Lu activity concentration in the tissue samples was presented as percentage of injected activity per gram:

$$c_{tissue}(t) = \frac{A_{tissue}(t)}{A_{inj} \cdot m_{tissue}} \cdot 100\ \%,$$

where A_{tissue} is the activity in the sample (time corrected to the time of injection), A_{inj} is the injected activity at time 0, and m_{tissue} is the sample weight.

3.4.1 Absorbed dose calculation (Papers II - IV)

Calculations of the absorbed dose to mouse bone marrow and GOT1 tumours were performed according to the Medical Internal Radiation Dose Committee (MIRD) formalism [96]:

$$D(r_T, T_D) = \frac{\tilde{A}(r_S, T_D)}{M(r_T)} \sum_i E_i Y_i \varphi(r_T \leftarrow r_S).$$

$\tilde{A}(_{r_S, T_D})$ is the time-integrated activity over the dose-integration period T_D in the source tissue r_S and $M_{(r_T)}$ is the mass of the target tissue r_T. $\sum_i E_i Y_i$ is the mean energy emitted per nuclear decay and was set to 148 keV [9], neglecting energy deposition by photons. The absorbed fraction, $\varphi(r_T \leftarrow r_S)$, was set to 1 for tumours and 0.738 for bone marrow [97] and source and target tissue was assumed to be the same $r_S = r_T$. Activity per tissue mass was obtained from previous biodistribution studies [98] and integration was done using the trapezoid function with assumption of zero activity at the start, A(r_S,0)=0.

Corresponding S values were used to calculate the absorbed dose to kidney cortex, kidney inner medulla and whole kidney [96]

$$D(r_T, T_D) = \tilde{A}(r_S, T_D) S(r_T \leftarrow r_S),$$

where $S(r_T \leftarrow r_S)$ is the absorbed dose rate in target tissue per unit activity in source tissue, and was obtained from literature [32] Data from previous biodistribution and activity measurements performed in the present study was used as basis for calculation of the time-integrated activity [98].

3.5 Gene expression analyses (Papers II and IV)

Total RNA was extracted from kidney medulla, kidney cortex and GOT1 tumour. RNA quality was evaluated with Nanodrop 1000 Spectrometer (Thermo Scientific, Waltham, Massachusetts, USA), RNA 6000 Nano LabChip Kit and Agilent 2100 Bioanalyzer (both Agilent Technologies, Santa Clara, Californian, USA) followed by RNA concentration measurement using Qubit 3.0 Fluorometer (Thermo Fisher Scientific, Waltham, Massachusetts, USA). The RNA was then reverse-transcribed into cDNA.

The gene expression in tumour tissue was analysed using RT-PCR array containing 84 human apoptosis related genes (QIAGEN, Hilden, Germany) and measured at TATAA Biocenter (Gothenburg, Sweden) using a Roche® LightCycler® 480 system (QIAGEN, Hilden, Germany). The gene expression in kidney tissue was analysed using corresponding array for mouse apoptosis related genes (QIAGEN, Hilden, Germany) measured in a 7500 Fast Real-Time PCR system (Applied Biosystems, Waltham, Massachusetts, USA).

Fold change (FC) compared with control was calculated using the $2^{-\Delta\Delta Ct}$ method [99] and converted to regulated FC by taking $\frac{-1}{FC}$ for FC values < 1. From here on regulated fold change is referred to as FC. Cut-off of $|FC| \geq 1.5$ followed by Welch's t-test ($p < 0.05$) was used to identify differentially expressed genes (DEGs). Statistically significant differences between the groups were determine by one-way ANOVA followed by Welch's t test ($p<0.05$).

Gene ontology (GO) terms were used to determine associated biological processes of the differentially expressed apoptosis-related genes. Cell death related GO terms for identified DEGs in GOT1 tumour and kidney tissue were obtained from AmiGO browse function (http://amigo.geneontology.org/amigo) and Mouse Genome Database (http://www.informatics.jax.org/), respectively. Gene expression data presented in this thesis have been deposited in NCBI's Gene Expression Omnibus database.

3.6 Proteomic analyses (Paper III)

Sample preparation and LC-MS/MS analysis was performed at the Proteomics Core Facility at Sahlgrenska Academy, University of Gothenburg, Sweden. Protein data presented in this thesis are available in the Proteomic identifications database (PRIDE).

Proteins from samples of mouse bone marrow, kidney medulla, and kidney cortex were extracted and digested with trypsin. Individual samples were used from treated mice and pooled samples from the control mice. A total of six TMT sets were used, each with pooled references for comparison between sets and between cortex and medulla. Peptide labelling were performed using TMT 11-plex isobaric mass tagging reagents (Thermo 204 Scientific, Waltham, Massachusetts, USA).

Mass spectrum of the peptide fractions were obtained using an Orbitrap Fusion Lumos Tribrid mass spectrometer interfaced with Easy-215 nLC1200 liquid chromatography system (both Thermo Scientific, Waltham, Massachusetts, USA). Identification and relative quantification was performed with Proteome Discoverer version 2.4 (Thermo Scientific, Waltham, Massachusetts, USA), searching against Mouse Swissprot Database version June 2019 (Swiss Institute of Bioinformatics, Switzerland) using search engine 235 Mascot 2.5 (Matrix Science, Chicago, Illinois, USA). For protein quantification, only unique peptides were considered and identified proteins were filtered at 1% false discovery rate.

FC was determined by dividing the protein abundance in treatment group with the abundance in control. A cut-off of $|FC| \geq 1.5$ was used to identify differentially expressed proteins (DRPs) and one-way ANOVA followed by Welch's t test (permutation based with 5% FDR) were used to determine statistically significant differences between the treatment groups.

Protein regulation data of identified DRP were analysed using Ingenuity Pathway Analysis (IPA) software version 51963813 (Qiagen, Hilden, Germany). IPA analysing tools were used to simulate affected canonical pathways, upstream regulators and toxicity functions. IPA uses Fisher's exact test (p-value ≤ 0.05) to compare observed regulation pattern in experimental data set with current biological knowledge using the Ingenuity® Knowledge Base. A z-score is used to predict activation state (compared with control) of identified canonical pathways, upstream regulators and biological functions, where $z \leq -2.0$ indicates inhibition and $z \geq 2.0$ indicates activation.

3.7 ELISA (Paper V)

Abcam (Cambridge, UK) ELISA kits was used to measure concentration of cystatin C, NGAL and RBP4 in mouse urine. Urinary creatinine was measured using ELISA kit from R&D Systems (Europe Ltd., Abingdon, UK). Optical density was measured using Perkin Elmer Victor 3 1420 Multilabel Plate Counter (Waltham, Massachusetts, USA).

IBM SPSS Statistics (version 25) linear mixed model with pairwise comparisons was used to determine if there were any statistically significant differences between any of the groups. The test was followed by IBM SPSS Statistics independent t-test to determine at which time-point the groups were statistically significant different.

3.8 Histopathological and immunohistochemical analyses (Paper V)

Kidneys were formalin fixed followed by paraffin embedding and sectioning. Some sections were stained with hematoxylin and eosin. Other kidney sections were first hybridized with S100A6, CDKN1A, ADIPOQ, NGAL and KIM-1 antibodies from Abcam (Cambridge, UK) and then stained with hematoxylin. A certified kidney pathologist performed histopathological analyses and evaluated the expression of the selected proteins.

4. Results and discussions

4.1 Impact of A1M on the therapeutic effects of ^{177}Lu-octreotate in tumours (Papers I-II)

At the start of this PhD project, very little was known about the effects of A1M on tumour tissue and possible interference with the anti-tumour effects of ^{177}Lu-octreotate. To ensure a preserved therapeutic effect of ^{177}Lu-octreotate when combined with A1M, potential changes in biodistribution and biokinetics of ^{177}Lu, tumour volume and regulation of apoptosis related genes in tumours were investigated.

4.1.1 Biodistribution of ^{177}Lu (Paper I)

The fundamental in treatment with ^{177}Lu-octreotate is the absorbed dose delivered by radiation emitted by ^{177}Lu, and the absorbed dose is directly dependent on the biodistribution and biokinetics of the radionuclide. When introducing alterations or addition to the treatment the biodistribution may be affected. In this thesis, changes in the biodistribution of ^{177}Lu were studied in GOT2-bearing mice after injection of ^{177}Lu-octreotate combined with A1M (referred to as rA1M in Paper I). In general, the biodistribution and biokinetics of ^{177}Lu after ^{177}Lu-octreotate injection were in agreement with previous published results using the same GOT2 tumour model [100]. No difference in activity concentration in any of the investigated organs were observed between mice injected with ^{177}Lu-octreotate alone or ^{177}Lu-octreotate and A1M (Paper I, Figure 1). Of special interest is that the ^{177}Lu activity concentration in GOT2 tumour tissue and kidneys remained unaffected.

4.1.2 Tumour volume reduction and re-growth (Paper I)

The effect of A1M on tumour remission and re-growth after ^{177}Lu-octreotate treatment was investigated in the GOT1 tumour model. A decrease in mean volume was observed for tumours in ^{177}Lu-octreotate and the combination group, with maximum decrease of 50% after about two weeks (Paper I, Figure 2). In the

combination group a slight delay in re-growth to original tumour mean volume was observed compare with re-growth of the tumours in the ^{177}Lu-octreotate group: 38 *versus* 31 days. However, during the time period when all mice still remained in the study (day 0 to day 21), there was no statistical significant difference in net change in tumour volume (Paper I, Figure 3).

4.1.3 Regulation of apoptosis related genes in tumour tissue (Paper II)

The expression of 84 genes related to apoptosis were investigated in GOT1 tumour tissue at 24 hours and 7 days after injection of ^{177}Lu-octreotate, ^{177}Lu-octreotate + A1M or A1M only. Overall, few of the investigated genes were differently expressed from control (identified as DEGs): 8 at day 1 and 14 at day 7 (Paper II, Figure 2, 3).

The apoptotic response at 24 hours was limited to the irradiated groups (the ^{177}Lu-octreotate and ^{177}Lu-octreotate + A1M group), and no DEGs were identified in the A1M group. Highest regulation among the DEGs were found for *FAS* and *TNFRSF10B*, both pro-apoptotic acting genes involved in the extrinsic pathway. Most of the genes related to pro-apoptotic processes were up-regulated indicating a pro-cell death response. At the same time-point downregulation of pro-apoptotic genes were also observed (*BAK1* and *BAD*) as well as upregulation of genes related to anti-apoptotic processes (*BCL2L2* and *BIRC3*). This indicates presence of both pro- and anti-cell death induction, but altogether, the gene expression in the irradiated GOT1 tumours at 24 hours can be interpreted as a pro-apoptotic response. At 7 days the pro-apoptotic response decreased; the number as well as the expression level of the pro-apoptotic DEGs were lower compared with the expression at 24 hours. The anti-apoptotic response was similar, or perhaps slightly increased. The opposite time dependence was observed in the A1M only group. No DEGs were observed at day 1, but at 7 days a total of 7 DEGs were observed, 6 pro-apoptotic DEGs (three downregulated and three upregulated) and 1 downregulated anti-apoptotic DEG. This complex response to A1M is interesting and should be further studied.

The decrease in pro-apoptotic response over time in irradiated groups are in agreement with our previous morphological studies with similar experimental design, GOT1 bearing mice injected with 30 MBq ^{177}Lu-octreotate [101]. That study demonstrated a decrease in apoptotic cell count from high levels at 1 and 3 days to low apoptotic cell count in the remaining tissue at 7 and 13 days post

injection. Considering these results together with the results of tumour volume reduction and gene expression in this thesis, it can be concluded that therapeutic effects of ^{177}Lu-octreotate on GOT1 tumours at least partly are due to radiation induced apoptosis.

At both time points, the general expression pattern, i.e. which genes that were affected (including genes not significant from control) and the direction of the regulation, in the combination group was similar to the pattern in the ^{177}Lu-octreotate group. These findings indicate that A1M does not alter the radiation induced regulation of apoptosis related genes in GOT1 tumours. An interesting exception is the strong downregulation of *BIRC5* in the combination group, statistically significant from all other groups. *BIRC5* is associated with anti-apoptotic processes and overexpression of *BIRC5* has previously been associated with radiation resistance during radiotherapy of different cancer types including gastrointestinal NETs [102-104]. It can be speculated that the radiosensitivity in NETs may increase when ^{177}Lu-octreotate is combined with A1M. Taken together with the results from the gene expression in the A1M only group, no indications of negative impact on radiation induced apoptosis were observed in GOT1 tissue when ^{177}Lu-octreotate were co-infused with A1M.

High expression ($|FC|>7$) was observed in some of the genes that were not found to be statistically significant from control (Paper II, Table 1). One example is the regulation of *TP73,* which was found to be highly upregulated in all groups at day 1. For some of these genes the RT-qPCR reading was unsuccessful resulting in loss of data that affects the statistical analysis. Biological variability between the GOT1 tumours, e.g. due to transplantation procedures and heterogeneous SSTR expression resulting in different absorbed dose, can also partly explain the large spread in expression for some of the investigated genes.

4.2 Early effects in kidney and bone marrow tissue (Papers III-IV)

A better understanding of the early radiobiological response in bone marrow and kidney to ^{177}Lu-octreotate exposure is most beneficial for radio protective purposes. In this work, the proteomic response to ^{177}Lu-octreotate was investigated in bone marrow and kidney as well as the regulation of selective apoptosis related genes in kidney. A comparison was made with the response when ^{177}Lu-octreotate and A1M was combined, and with A1M alone.

4.2.1 Effects of ^{177}Lu-octreotate (Papers III-IV)

Regulation of apoptosis related genes were observed in kidney tissue early (1 ad 7 days) after injection of ^{177}Lu-octreotate. A total of 11 different DEGs were observed, most of them are related to pro-apoptotic processes and were upregulated (Paper IV, Figures 2-3). These findings indicate that apoptosis may be induced in both kidney medulla and kidney cortex following ^{177}Lu-octreotate exposure. However, only three DEGs (*Bax*, *Bcl2l1*, and *Tnfrsf10b*) were common to the two tissue types, showing a certain tissue dependence in the affected apoptosis related genes. In kidney cortex, four DEGs were observed at both time points: *Apaf1, Bax, Tnfrsf10b* and *Casp1* (Paper IV, Figure 2). *Bax* was the only DEG observed to be regulated at both time points in kidney medulla (Paper IV, Figure 3). High regulation ($|FC| > 5$) in DEGs were found for *Tnfrsf10b* in both tissue types and *Cd40lg* in cortex. In general, less regulation, both in number of regulated genes and level of regulation, were observed at 7 days compared to 24 hours.

The proteomics analysis of kidney tissue identified 130 DRPs in medulla and 74 in cortex, 24 h after injection of ^{177}Lu-octreotate (Figure 4.1). At 7 days 85 DPRs were observed in medulla and 108 in cortex (Figure 4.1). In medulla, about 75% of the DPRs were downregulated. Only three ^{177}Lu-octreotate unique DRPs were found among the highly regulated proteins in kidney tissue: KRT82, KRT31 and KRT85, all of them hair keratin proteins (Paper III, Table 1). BAX, EPHX1, PFET1, MGMT and PHLDA3 are among the most recurrently identified DEGs found in both kidney tissue types and/or at both time points. Transcripts of EPHX1 and PHLDA3 have been found to be regulated in our previous transcript study with similar experimental design [90] and BAX is one of the most recurrently regulated apoptosis related genes observed in this thesis work (Paper IV, Figures 2-3). *BAX* and *PHLDA3* genes have previously been identified as radiation

responsive genes and have been suggested as radiation biomarkers [105]. BBC3 (also known as PUMA), is another protein of previously identified radiation responsive genes that was found to be regulated in kidney medulla after ^{177}Lu-octreotate exposure [105-107].

It may be surprising that so few of the regulated apoptosis related genes in this thesis were observed at the protein level. However, low correlation between gene and protein expression have been shown in previous studies, including our previous studies on transcript and protein regulation with similar experimental design [90, 91]. Suggested reasons for the lack of agreement in gene and protein expression data include translational efficiency, variability in mRNA expression over the cell cycle and the half-life of the mRNA and the protein [108].

The total number of identified DRPs in bone marrow were 70 at 24 hours and 87 at 7 days after ^{177}Lu-octreotate injection, most of them downregulated (Figure 4.1). Few DRPs were only found in the ^{177}Lu-octreotate group, about 50 % of the DRPs were common for all three groups (Paper III, Figure 1).

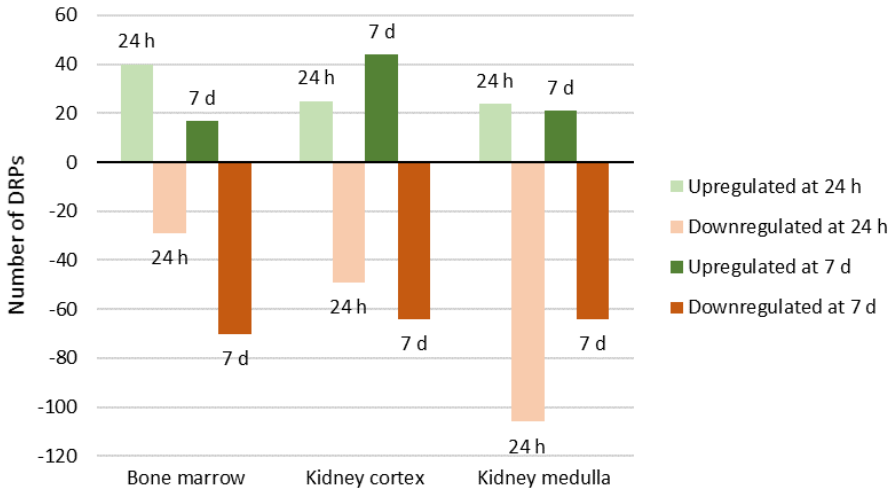

Figure 4.1 Total number of differentially regulated proteins in mouse tissues 24 hours and 7 days after injection of 150 MBq ^{177}Lu-octreotate. Green bars (positive numbers) shows the number of upregulated proteins (FC ≥ 1.5) and red bars (negative numbers) shows the number of downregulated proteins (FC ≤ -1.5) in Paper III.

In summary, apoptosis related genes were regulated in kidney tissue early after ^{177}Lu-octreotate injection. The proteomic response to ^{177}Lu-octreotate seems to be

tissue specific. Proteins of previously identified radiation responsive genes were regulated in kidney. A lesser proteomic response to ^{177}Lu-octreotate was observed in bone marrow. This is surprising since the bone marrow is a radio sensitive and fast responding organ. It can be speculated that this high single dose of ^{177}Lu-octreotate (150 MBq) induced higher degree of cell death in bone marrow and that the surviving cells in the kidney give a higher proteomic response due to induction of repair mechanisms.

4.2.2 Effects of A1M (Papers III-IV)

Of the 84 investigated apoptosis related genes, 13 were found to be significantly regulated in kidney tissue short-time after injection of A1M (Paper IV, Figure 2-3). Interestingly, 11 of them were observed in kidney medulla at 7 days, all of them downregulated compared with control. The GO annotations of these genes show that they previously been associated with pro-cell death processes or both pro and anti-cell death processes (Paper IV, Supplemental table 1). Since all of them were downregulated, this can be interpreted as an anti-apoptotic response was induced in kidney medulla after injection of A1M. None of the genes were differently expressed in medulla at 24 h, indicating that the anti-apoptotic response was time dependent.

The proteomics analysis of kidney tissue identified 127 DRPs in medulla and 70 in cortex, 24 h after injection of A1M (Figure 4.2). At 7 days 105 DPRs were observed in medulla and 93 in cortex (Figure 4.2). Eight highly expressed DRPs in kidney tissue were found to be unique for the A1M group; ARHGAP23, LCN2, CHIL3 and TGFB1I1 in medulla and KV2A7, KV3A8, S100A9, and IGHG1 in cortex (Paper III, Table 1). Many of the highly upregulated DRPs in kidney tissue are related to immune and inflammatory responses, e.g. LCN2, S100A9 and SAA1. These findings could indicate an immunologic and inflammatory response by A1M exposure, which is not in agreement with previous studies describing A1M as immunosuppressive and anti-inflammatory [109].

In bone marrow 125 DRPs were observed at 24 hours after A1M injection and at 7 days the number of DRPs had increased to 325 (Figure 4.2), where most were either shared with the combination group or unique for the A1M group (Paper III, Figure 1). Among the highly expressed DRPs in bone marrow, two DRPs were unique for the A1M group: IGHG1 and PTMS (Paper III, Table 1). A1M has previously been reported to interact with red blood cells contributing to stabilisation and protection from haemolysis [62, 109-111]. These properties

could partly explain the much stronger proteomic response after A1M injection observed in bone marrow compared with kidney tissue.

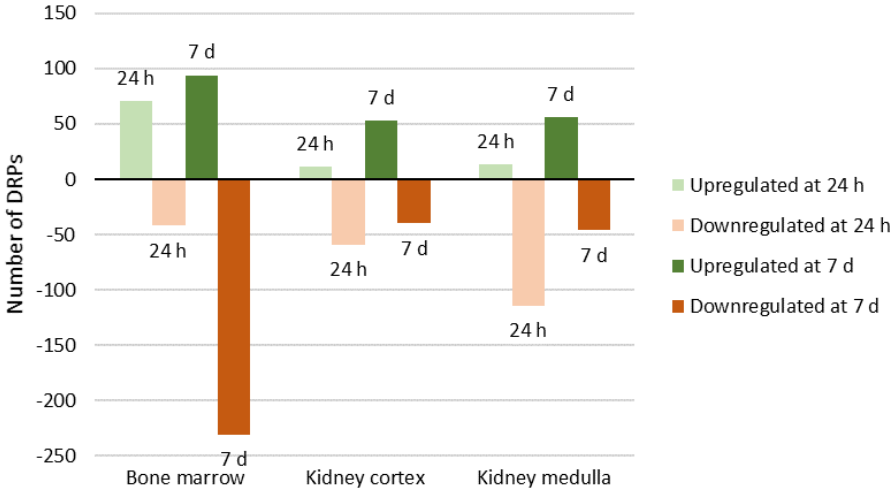

Figure 4.2 Total number of differentially regulated proteins in mouse tissues 24 hours and 7 days after injection of A1M. Green bars (positive numbers) shows the number of upregulated proteins (FC ≥ 1.5) and red bars (negative numbers) shows the number of downregulated proteins (FC ≤ -1.5) in Paper III.

In summary, the observed response to A1M in normal tissue short time after injection seems to increase with time. A1M has a short life-time and it is not likely that any significant amount of the infused A1M is left in the blood or tissue as late as 7 days after injection. The anti-apoptotic response in kidney medulla and the increased protein regulation in bone marrow at 7 days is therefore likely a consequence of processes stimulated by the infused A1M. What these processes are and how they are initiated remains to be further investigated.

4.2.3 Effects of ^{177}Lu-octreotate combined with A1M (Papers III-IV)

Twelve of the 84 investigated apoptosis related genes were found to be significantly regulated in kidney after injection of ^{177}Lu-octreotate + A1M (Paper IV, Figures 2-3). Six DEGs were observed at 24 hours and nine at 7 days with three DEGs found at both time points (*Apaf1, Bax* and *Tnfrsf10b)*. In cortex, the general expression pattern was relatively unchanged when ^{177}Lu-octreotate was combined with A1M. Seven DEGs were detected and out of them five were also

observed in the ^{177}Lu-octreotate group: *Apaf1, Bax, Bcl2l1, Casp3* and *Tnfrsf10b*. Statistically significant differences in regulation between the groups were found for *Bax* and *Casp1*, both at 24 hours. Similar to the ^{177}Lu-octreotate group, the regulation of the apoptosis related genes in cortex showed a slight decrease with time. In medulla, differences in the general expression pattern between the combination group and the ^{177}Lu-octreotate only group were more profound. Three DEGs were observed at 24 hours (*Bax, Casp4* and *Tnfrsf10b),* where the expression of *Casp4* was statistically significant higher than in the ^{177}Lu-octreotate group. *Tnfrsf10b* was also regulated at 7 days after injection of ^{177}Lu-octreotate + A1M, along with 6 other genes, none of them significantly regulated in the ^{177}Lu-octreotate group. *Bok* was the highest regulated DEG in medulla: downregulated (FC = -6.0, SEM = 0.1) at 7 days after injection of ^{177}Lu-octreotate + A1M.

At 24 h after injection of ^{177}Lu-octreotate and A1M, a total of 93 and 110 DRPs were identified in kidney cortex and kidney medulla, respectively (Figure 4.3). A slight increase in the number of DRPs were observed at 7 days: 127 DPRs in medulla and 136 in cortex (Figure 4.3). Most of the DRPs in kidney medulla were downregulated. The proportion of proteins unique to the ^{177}Lu-octreotate + A1M group increased over time and were about 40-50 % at 7 days (Paper III, Figure 1). Two highly expressed DRPs were unique for the combination group: THRSP and EDRF1, both upregulated at 7 days in kidney cortex (Paper III, Table 1).

In bone marrow, a large increase in the total number of DRPs was observed with time after injection of ^{177}Lu-octreotate and A1M (Figure 4.3). At 24 hours 139 DRPs were observed and about 45 % were unique for the combination group. At 7 days the number of DRPs had increased to 230 (Paper III, Figure 1) with great agreement with the A1M group; about 60 % of the DRPs were shared with the A1M group. Five highly expressed DRPs were unique for the combination group: ACTN2, CRYAB, HSPB6, KRT6A and MYH7, most of them found at 24 hours.

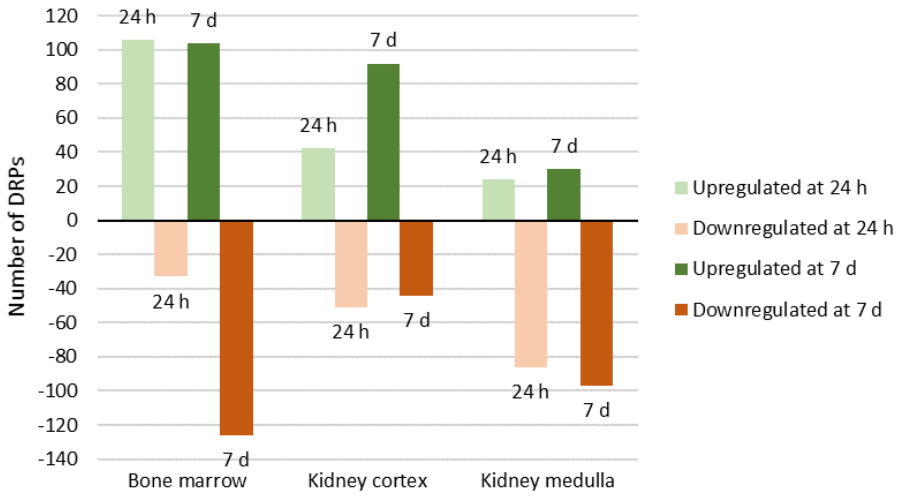

Figure 4.3 Total number of differentially regulated proteins in mouse tissues 24 hours and 7 days after injection of 150 MBq ^{177}Lu-octreotate + A1M. Green bars (positive numbers) shows the number of upregulated proteins (FC ≥ 1.5) and red bars (negative numbers) shows the number of downregulated proteins (FC ≤ -1.5) in Paper III.

Similar to the ^{177}Lu-octreotate group, BAX, EPHX1, MGMT and PHLDA3 are among the most recurrently identified DEGs in the combination group found in both kidney tissue types and/or at both time points. Many of the radiation related proteins found in the ^{177}Lu-octreotate group were also found in the combination group: BAX, BBC3 and PHLDA3, in addition to HP and SAA1 that were regulated in the combination group, but not in the ^{177}Lu-octreotate group (Figure 4.4). No statistically significant difference in regulation of BAX, BBC3 and PHLDA3 was observed between the combination and the ^{177}Lu-octreotate groups in any of the tissues or time points. Statistically significant difference in the regulation of SAA1 and HP was observed; both proteins were upregulated in kidney cortex at 24 hours after injection of ^{177}Lu-octreotate + A1M, but not after injection of ^{177}Lu-octreotate alone. In humans, SAA proteins are associated with inflammation and elevated serum levels of SAA1 have been observed in both humans and mice following irradiation [107, 112]. In this thesis work, upregulation of SAA1 (and SAA2) was also observed in the A1M group, indicating that the regulation may be a response to A1M and not the irradiation. Radiation induced over expression of HP has previously been found in bone marrow [107, 113, 114]. The regulation of HP in this thesis work seems to be a response to a combination of radiation and A1M rather than a response to the irradiation by itself. Since both A1M and HP are known to protect tissue from

harmful levels of hemoglobin and heme [66, 115], it could be speculated that infusion of A1M stimulates activation of these defence mechanisms, by upregulation of HP.

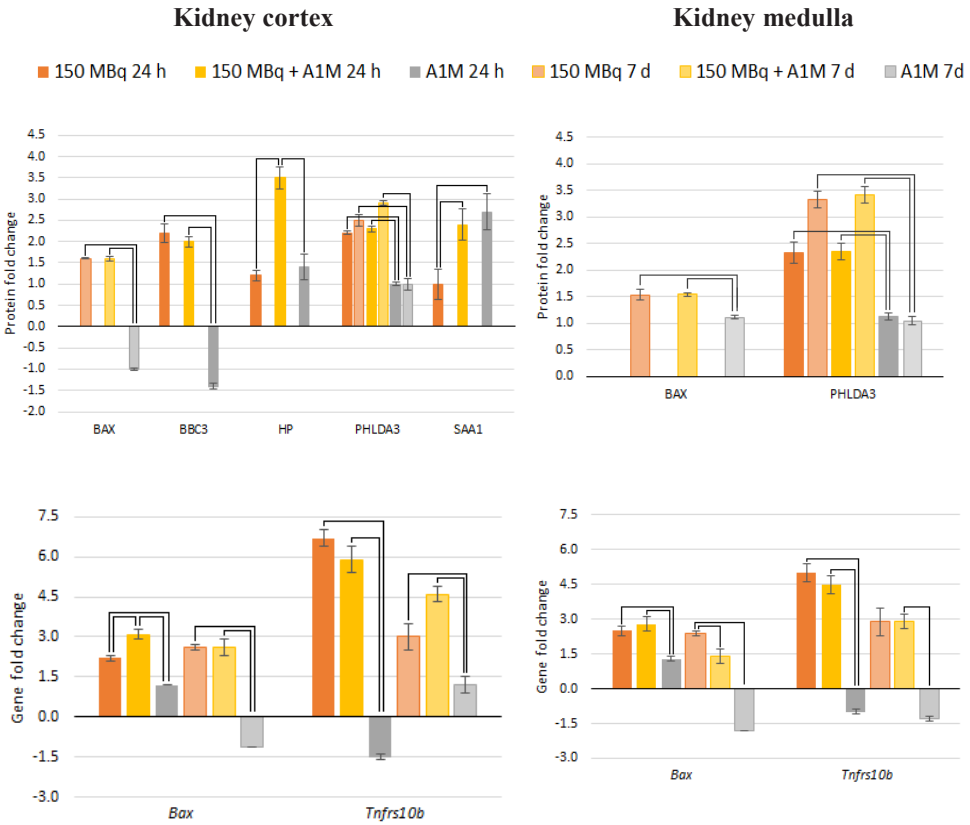

Figure 4.4 Regulation of radiation associated proteins (Paper III) and genes (Paper IV) with significant regulation compared with control (|FC| ≥ 1.5) in kidney tissue at 24 hours or 7 days after injection of 150 MBq ^{177}Lu-octreotate, 150 MBq ^{177}Lu-octreotate with A1M, or with A1M alone. Error bars show SEM and brackets show statistically significant differences between the groups.

Two of the apoptosis related DEGs (*Bax* and *Tnfrs10b*) observed in kidney tissue after injection of ^{177}Lu-octreotate with or without A1M have previously been described as "highly reproducible radiation-responsive genes" [105] (Figure 4.4). No statistically significant difference in the regulation of *Tnfrs10b* was observed between the two irradiated groups. Some changes in the regulation of *Bax* were observed when ^{177}Lu-octreotate was combined with A1M: higher regulation in cortex at 24 hours and lower regulation in medulla at 7 days.

In summary, no major differences in regulation of apoptosis related genes or radiation responsive proteins were observed in kidney tissue when ^{177}Lu-octreotate was combined with A1M. A general increase in number of regulated proteins were observed over time, especially in bone marrow. The number of unique and shared proteins indicated similarity between the ^{177}Lu-octreotate group and the combination group in kidney tissue, whereas in bone marrow higher agreement was observed between the A1M and the combination group.

4.3 Long-term effects in normal tissue (Paper V)

Better methods for prediction of renal damage following ^{177}Lu-octreotate are needed to optimise the treatment. Reliable early responding biomarkers may improve the possibility to adapt the treatment to the individual patient and to identify which patients that safely can be given a higher total amount of administered activity. In this work, evaluation of previously proposed biomarkers for renal damage was performed in urine and kidney from mice injected with ^{177}Lu-octreotate. The results were compared with corresponding results from mice co-administered with ^{177}Lu-octreotate and A1M.

4.3.1 Morphological signs of kidney injury (Paper V)

Signs of kidney injury were seen in the histological evaluation of mouse kidneys, 9 months after injection of 150 MBq ^{177}Lu-octreotate (Paper V, Figure 4). Dilation of the pelvis and reduction of the cortical thickness was observed. No significant changes in glomerular morphology were detected, but severe damages were seen in the tubules with on average 75% tubular atrophy and fibrosis. No significant signs of tubular or glomerular injury were observed for the lower activity level, 90 MBq ^{177}Lu-octreotate and no histological changes were seen in kidneys from mice injected with A1M alone (Paper V, Figure 4). Severe effects on the kidneys have previously been observed in rat and nude mice following ^{177}Lu-octreotate exposure [32, 116, 117]. In those studies, effects were primarily observed in proximal tubules with only mild effects on glomerulus. These findings are well in line with the morphological signs of kidney injury found in this thesis. In our previous studies with similar experimental design as in this work (same mouse model, activity levels and similar time point) morphological changes were mainly observed in glomerulus and not in the tubules [92]. The reason for this controversy is not known, and should be studied further.

No mitigating effect on the kidney damage was seen in mice that received injection of 150 MBq ^{177}Lu-octreotate in addition to A1M (Paper V, Figure 4). This stands in contrast to the findings of Kristiansson A *et. al* [73], who observed less effects in mouse kidney at 24 weeks post injection when 150 MBq ^{177}Lu-octreotate was combined with 5 mg/kg A1M. In that study, fewer kidney lesions (not statistically significant) and statistically significant higher glomeruli counts were found in the combination group compared to the ^{177}Lu-octreotate group.

4.3.2 Biomarkers for kidney damage (Paper V)

Among the investigated urinary biomarkers for kidney damage, RBP4, which is related to tubular damage, was the earliest responding one with elevated levels from 35 days after injection of 150 MBq ^{177}Lu-octreotate (Paper V, Figures 2-3). These results confirm our previous observation of elevated levels of urinary RBP4 in mice from day 30 after injection of 60 or 120 MBq ^{177}Lu-octreotate [87]. In the present study indications of reduced GFR were also observed in the irradiated mice, by significant change in urinary levels of cystatin C and creatinine at the later time points (day 131 and 223) (Paper V, Figures 2-3). No significant change was observed in urinary NGAL in any of the groups or time points, making it less suitable as biomarker for ^{177}Lu-octreotate induced kidney damage. No statistically significant difference was observed in level of urinary biomarkers in the comparison between mice injected with ^{177}Lu-octreotate and mice injected with ^{177}Lu-octreotate and A1M (Paper V, Figures 2-3). Even so, the levels of RBP4 and cystatin C differed to a greater extent from control in the ^{177}Lu-octreotate group than the combination group. This trend is however unclear due to large variation in individual response in mice within the groups.

The immunohistochemical analyses showed increased expression of NGAL, KIM-1, CDKN1A and S100A6 compared to controls in mouse kidneys 9 months after injection of ^{177}Lu-octreotate. Only slightly elevated ADIPOQ expression was observed. The expression of KIM-1, CDKN1A and S100A6 was dose-dependent: slightly higher expression in kidneys after injection of 90 MBq ^{177}Lu-octreotate (compared to control) and even higher expression after injection of 150 MBq ^{177}Lu-octreotate. The ^{177}Lu-octreotate induced expression of the investigated histological markers was in general unaffected by co-administration of A1M.

In summary, RBP4 is a promising early responding urinary biomarker for ^{177}Lu-octreotate induced kidney damage, and KIM-1, CDKN1A and S100A6 may be

suitable immunohistochemical markers. Signs of kidney damage by these markers were in general unaffected by co-administration of A1M.

5. Conclusions

Conclusions from investigation of the potential influence of A1M on the therapy effect of ^{177}Lu-octreotate in NET mouse models can be summarized as follows:

- co-administration of ^{177}Lu-octreotate and A1M did not change the biodistribution of ^{177}Lu in GOT2 NET bearing mice compared with that of ^{177}Lu-octreotate **(Paper I)**
- co-administration of ^{177}Lu-octreotate and A1M had no negative effects on the ^{177}Lu-octreotate induced change in GOT1 NET volume **(Paper I)**
- expression of genes related to apoptosis were detected in GOT1 NET 1 and 7 days after ^{177}Lu-octreotate injection **(Paper II)**
- co-administration with A1M resulted in a similar transcriptional apoptotic response as ^{177}Lu-octreotate alone in GOT1 NET **(Paper II)**
- A1M alone did not significantly affect apoptotic gene regulation in GOT1 NET **(Paper II)**

Conclusions from investigation of molecular biological effects in normal mouse kidney and bone marrow short time after administration of ^{177}Lu-octreotate with or without A1M and A1M alone can be summarized as follows:

- proteomic response after exposure to ^{177}Lu-octreotate with or without A1M and A1M alone was tissue-dependent with different response patterns in bone marrow, kidney medulla and kidney cortex **(Paper III)**
- previously observed radiation responsive proteins were found to be regulated in kidney medulla and kidney cortex after administration of ^{177}Lu-octreotate, and co-administration with A1M did not in general alter the regulation of these proteins **(Paper III)**
- expression of genes related to apoptosis following exposure to ^{177}Lu-octreotate depended on kidney tissue region (cortex *versus* medulla) **(Paper IV)**
- indications of pro-survival response to A1M were observed in the regulation of apoptosis related genes in kidney medulla **(Paper IV)**

Based on evaluation of urinary biomarkers and kidney expression of protein markers of toxicity, biomarkers for ^{177}Lu-octreotate induced kidney damage were proposed:

- urinary RBP4 is a promising early responding biomarker for ^{177}Lu-octreotate induced late kidney damage **(Paper V)**
- KIM-1, CDKN1A and S100A6 are promising biomarkers for ^{177}Lu-octreotate induced kidney injury **(Paper V)**

No clear protective effect of A1M on ^{177}Lu-octreotate induced effects on the proposed biomarkers or morphological changes observed in kidneys.

6. Future perspectives

The results in this thesis demonstrated no negative effects of A1M on ^{177}Lu-octreotate treatment of the two NET models, GOT1 and GOT2. To get a better understanding of how the radioprotective effects of A1M influences tumours the co-localisation of ^{177}Lu and A1M after injection of ^{177}Lu-octreotate together with A1M needs to be studied in tumour tissue. Furthermore, different antioxidants have different effects and the impact of supplements of antioxidant may vary between different types of cancer and also between subtypes within a cancer group. It is therefore of interest to repeat the investigation of A1Ms effect on tumour tissue using other NETs or NET-like models *in vivo*.

No clear radioprotective effect of A1M on kidneys were detected when ^{177}Lu-octreotate were combined with A1M. A possible explanation may be that the A1M administration protocol, used in all studies included in this thesis, is suboptimal. Further studies are therefore important to investigate effects of timing and number of A1M administration, including effects in both tumour and normal tissues.

The effects of ^{177}Lu-octreotate in combination with A1M have until now not been studied in bone marrow. Proteomic findings in this thesis indicate that A1M has an effect on irradiated as well as non-irradiated bone marrow. These findings along with haematological toxicity needs to be validated and studied further.

Apoptosis is considered to be one of the main cell death processes after irradiation. A better understanding of radiation induced apoptosis can be useful for optimisation of radionuclide therapy, either with the goal to increase cell death in tumours or to achieve the opposite in normal tissues. More studies should be conducted to understand the differences in radiation induced apoptosis mechanisms in different tissue types. Furthermore, relation between apoptotic response and irradiation related factors such as dose, dose-rate and type of radiation should be more extensively studied. The findings of regulated apoptosis related genes in this thesis contributes to an increased knowledge about ^{177}Lu induced apoptosis. However, the number of investigated genes were limited and some previously observed radiation responsive apoptosis genes were not included among the pre-selected genes, e.g. BBC3 (also known as PUMA). Further

investigations should include more radiation responsive genes as well as validation of key finding on protein level with e.g. Western blot and IHC.

The proposed urinary biomarker RBP4 needs to be tested and validated in patients undergoing ^{177}Lu-octreotate treatment. Urinary samples should be collected at different time points after treatment. The biomarker levels should be correlated with the absorbed dose to the kidneys based on individual kidney dosimetry, together with long term follow-up of kidney function.

There are still gaps of knowledge on how or if different antioxidants can be effective and safe to use as radioprotectors of normal tissues in radionuclide cancer treatments. Further studies are needed to investigate combinations of different types of antioxidants, and radiopharmaceuticals and types of side effects in critical organs. Filling these gaps of knowledge would be most valuable for optimisation of future cancer treatments in the future.

Acknowledgements

I would like to take this opportunity to thank, in no particular order, the following people who in different ways have helped me through this process.

My supervisor **Eva Forssell-Aronsson,** for trusting me and believing in me, especially at times when I had a hard time doing the same for myself. I will forever be grateful for everything you have taught me about research and life in general.

My co-supervisor **Khalil Helou**, for sharing your great knowledge in molecular biology. Thank you for all the times you have helped me with my endless questions.

My closest group of present and former colleagues whom I enjoyed sharing all the work and adventures with: **Amin Al-Awar, Ann Wikström, Arman Romiani, Hana Bakr, Klara Insulander Björk, Lukas Lundholm, Malin Larsson, Mikael Elvborn, Mikael Montelius, Sofia Saadati** and **Viktor Sandblom**. Special thanks to **Britta Langen** and **Johan Spetz**, for being a great support early in my PhD studies and for showing me what good lab practise looks like. I owe you so much! Thank you **Emman Shubbar** and **Daniella Pettersson**, your skills, commitment and kindness have made all the late hours at the animal facility so much more enjoyable. Thank you **Nishte Rassol**, you are a true source of inspiration and I am privileged to have taken part in the beginning of your research studies.

My colleagues at the Department of Medical Radiation Sciences and Sahlgrenska Centre for Cancer Research, especially **Jennie Bengtsson** and **Maria Andersson** for the company and all the different workout opportunities you have given me. **Ella Ittner, Maxim Olsson, Peter Larsson** and **Toshima Parris** for all the times you have helped me out in the lab and for all the nice and interesting lunches. Also a thanks to all the construction workers who have kept me entertained during incubation times in the lab. During the time it has taken me to complete this thesis, you have dismantled a hill and replaced it with a building.

My previously unmentioned co-authors: **Bo Åkerström, Britt-Marie Olsson, Emil Schüler, Klara Simonsson, Magnus Gram, Martin Johansson** and

Sven-Erik Strand. Thank you for your valuable contributions, it has been a pleasure working with you.

My fellow young researchers and peers in the PhD Student group at the Department of Medical Radiation Sciences, the PhD Student Council at the Sahlgrenska Academy and the Swedish Radiation Research Association for young Scientists. Thank you for all the fun we've had!

My loved ones: my family and friends who have been so supportive! Special thanks to **Elias** and **Ida**, for all the times you have listened to me go on and on about work and for reminding me to celebrate all the successes!

References

1. Forssell-Aronsson, E., et al., *Biodistribution data from 100 patients i.v. injected with 111In-DTPA-D-Phe1-octreotide.* Acta Oncol, 2004. **43**(5): p. 436-42.
2. Forssell-Aronsson, E.B., et al., *111In-DTPA-D-Phe1-octreotide binding and somatostatin receptor subtypes in thyroid tumors.* J Nucl Med, 2000. **41**(4): p. 636-42.
3. de Jong, M., et al., *Comparison of (111)In-labeled somatostatin analogues for tumor scintigraphy and radionuclide therapy.* Cancer Res, 1998. **58**(3): p. 437-41.
4. Valkema, R., et al., *Phase I study of peptide receptor radionuclide therapy with [In-DTPA]octreotide: the Rotterdam experience.* Semin Nucl Med, 2002. **32**(2): p. 110-22.
5. Fjälling, M., et al., *Systemic radionuclide therapy using indium-111-DTPA-D-Phe1-octreotide in midgut carcinoid syndrome.* J Nucl Med, 1996. **37**(9): p. 1519-21.
6. Forssell-Aronsson, E., et al., *Indium-111 activity concentration in tissue samples after intravenous injection of indium-111-DTPA-D-Phe-1-octreotide.* J Nucl Med, 1995. **36**(1): p. 7-12.
7. Uusijärvi, H., P. Bernhardt, and E. Forssell-Aronsson, *Translation of dosimetric results of preclinical radionuclide therapy to clinical situations: influence of photon irradiation.* Cancer Biother Radiopharm, 2007. **22**(2): p. 268-74.
8. Bakker, W.H., et al., *Iodine-131 labelled octreotide: not an option for somatostatin receptor therapy.* Eur J Nucl Med, 1996. **23**(7): p. 775-81.
9. Eckerman K, E.A., *ICRP Publication 107. Nuclear decay data for dosimetric calculations*. 2008. p. 7-96.
10. Kwekkeboom, D.J., et al., *Treatment with the radiolabeled somatostatin analog [177 Lu-DOTA 0,Tyr3]octreotate: toxicity, efficacy, and survival.* J Clin Oncol, 2008. **26**(13): p. 2124-30.
11. Waldherr, C., et al., *Tumor response and clinical benefit in neuroendocrine tumors after 7.4 GBq (90)Y-DOTATOC.* J Nucl Med, 2002. **43**(5): p. 610-6.
12. Kwekkeboom, D.J., et al., *Somatostatin-receptor-based imaging and therapy of gastroenteropancreatic neuroendocrine tumors.* Endocr Relat Cancer, 2010. **17**(1): p. R53-73.
13. Vegt, E., et al., *Renal toxicity of radiolabeled peptides and antibody fragments: mechanisms, impact on radionuclide therapy, and strategies for prevention.* J Nucl Med, 2010. **51**(7): p. 1049-58.

14. Cremonesi, M., et al., *Correlation of dose with toxicity and tumour response to (90)Y- and (177)Lu-PRRT provides the basis for optimization through individualized treatment planning.* Eur J Nucl Med Mol Imaging, 2018. **45**(13): p. 2426-2441.
15. Bodei, L., et al., *Long-term tolerability of PRRT in 807 patients with neuroendocrine tumours: the value and limitations of clinical factors.* Eur J Nucl Med Mol Imaging, 2015. **42**(1): p. 5-19.
16. Strosberg, J., et al., *Phase 3 Trial of (177)Lu-Dotatate for Midgut Neuroendocrine Tumors.* N Engl J Med, 2017. **376**(2): p. 125-135.
17. *Authorization details for Lutathera® in Europe*. [cited 2022 April 19]; Available from: https://www.ema.europa.eu/en/medicines/human/EPAR/lutathera#authorisation-details-section.
18. *LUTATHERA® Summary of Product Characteristics*. [cited 2020 February 21]; Available from: https://www.ema.europa.eu/en/documents/product-information/lutathera-epar-product-information_en.pdf.
19. Bodei, L., et al., *Peptide receptor radionuclide therapy with ^{177}Lu-DOTATATE: the IEO phase I-II study.* Eur J Nucl Med Mol Imaging, 2011. **38**(12): p. 2125-35.
20. Swärd, C., et al., *[177Lu-DOTA 0-Tyr 3]-octreotate treatment in patients with disseminated gastroenteropancreatic neuroendocrine tumors: the value of measuring absorbed dose to the kidney.* World J Surg, 2010. **34**(6): p. 1368-72.
21. Garske-Román, U., et al., *Prospective observational study of (177)Lu-DOTA-octreotate therapy in 200 patients with advanced metastasized neuroendocrine tumours (NETs): feasibility and impact of a dosimetry-guided study protocol on outcome and toxicity.* Eur J Nucl Med Mol Imaging, 2018. **45**(6): p. 970-988.
22. Forssell-Aronsson, E., J. Spetz, and H. Ahlman, *Radionuclide therapy via SSTR: future aspects from experimental animal studies.* Neuroendocrinology, 2013. **97**(1): p. 86-98.
23. Sundlöv, A., et al., *Individualised (177)Lu-DOTATATE treatment of neuroendocrine tumours based on kidney dosimetry.* Eur J Nucl Med Mol Imaging, 2017. **44**(9): p. 1480-1489.
24. Brabander, T., J. Nonnekens, and J. Hofland, *The next generation of peptide receptor radionuclide therapy.* Endocr Relat Cancer, 2019. **26**(8): p. C7-c11.
25. Geenen, L., et al., *Overcoming nephrotoxicity in peptide receptor radionuclide therapy using [(177)Lu]Lu-DOTA-TATE for the treatment of neuroendocrine tumours.* Nucl Med Biol, 2021. **102-103**: p. 1-11.
26. Melis, M., et al., *Localisation and mechanism of renal retention of radiolabelled somatostatin analogues.* Eur J Nucl Med Mol Imaging, 2005. **32**(10): p. 1136-43.
27. Reubi, J.C., et al., *Affinity profiles for human somatostatin receptor subtypes SST1-SST5 of somatostatin radiotracers selected for*

scintigraphic and radiotherapeutic use. Eur J Nucl Med, 2000. **27**(3): p. 273-82.
28. Bhandari, S., et al., *Expression of somatostatin and somatostatin receptor subtypes 1-5 in human normal and diseased kidney.* The journal of histochemistry and cytochemistry : official journal of the Histochemistry Society, 2008. **56**(8): p. 733-743.
29. Bates, C.M., H. Kegg, and S. Grady, *Expression of somatostatin in the adult and developing mouse kidney.* Kidney International, 2004. **66**(5): p. 1785-1793.
30. Bates, C.M., H. Kegg, and S. Grady, *Expression of somatostatin receptors 1 and 2 in the adult mouse kidney.* Regul Pept, 2004. **119**(1-2): p. 11-20.
31. Bates, C.M., et al., *Expression of somatostatin receptors 3, 4, and 5 in mouse kidney proximal tubules.* Kidney Int, 2003. **63**(1): p. 53-63.
32. Svensson, J., et al., *Nephrotoxicity profiles and threshold dose values for [177Lu]-DOTATATE in nude mice.* Nucl Med Biol, 2012. **39**(6): p. 756-62.
33. Melis, M., et al., *Renal uptake and retention of radiolabeled somatostatin, bombesin, neurotensin, minigastrin and CCK analogues: species and gender differences.* Nucl Med Biol, 2007. **34**(6): p. 633-41.
34. De Jong, M., et al., *Inhomogeneous localization of radioactivity in the human kidney after injection of [(111)In-DTPA]octreotide.* J Nucl Med, 2004. **45**(7): p. 1168-71.
35. Rolleman, E.J., et al., *Safe and effective inhibition of renal uptake of radiolabelled octreotide by a combination of lysine and arginine.* Eur J Nucl Med Mol Imaging, 2003. **30**(1): p. 9-15.
36. Rolleman, E.J., et al., *Molecular imaging of reduced renal uptake of radiolabelled [DOTA0,Tyr3]octreotate by the combination of lysine and Gelofusine in rats.* Nuklearmedizin, 2008. **47**(3): p. 110-5.
37. Reisz, J.A., et al., *Effects of ionizing radiation on biological molecules--mechanisms of damage and emerging methods of detection.* Antioxidants & redox signaling, 2014. **21**(2): p. 260-292.
38. Mishra, K.N., B.A. Moftah, and G.A. Alsbeih, *Appraisal of mechanisms of radioprotection and therapeutic approaches of radiation countermeasures.* Biomed Pharmacother, 2018. **106**: p. 610-617.
39. Prise, K.M., et al., *New insights on cell death from radiation exposure.* Lancet Oncol, 2005. **6**(7): p. 520-8.
40. Prise, K.M. and J.M. O'Sullivan, *Radiation-induced bystander signalling in cancer therapy.* Nat Rev Cancer, 2009. **9**(5): p. 351-60.
41. Bright, S. and M. Kadhim, *The future impacts of non-targeted effects.* Int J Radiat Biol, 2018. **94**(8): p. 727-736.
42. Hei, T.K., et al., *Radiation induced non-targeted response: mechanism and potential clinical implications.* Current molecular pharmacology, 2011. **4**(2): p. 96-105.

43. Wei, J., et al., *Radiation-Induced Normal Tissue Damage: Oxidative Stress and Epigenetic Mechanisms.* Oxid Med Cell Longev, 2019. **2019**: p. 3010342.
44. Philchenkov, A., *Radiation-Induced Cell Death: Signaling and Pharmacological Modulation.* Crit Rev Oncog, 2018. **23**(1-2): p. 13-37.
45. Eriksson, D. and T. Stigbrand, *Radiation-induced cell death mechanisms.* Tumour Biol, 2010. **31**(4): p. 363-72.
46. Galluzzi, L., et al., *Molecular mechanisms of cell death: recommendations of the Nomenclature Committee on Cell Death 2018.* Cell Death & Differentiation, 2018. **25**(3): p. 486-541.
47. Verburg, F.A., et al., *To go where no one has gone before: the necessity of radiobiology studies for exploration beyond the limits of the "Holy Gray" in radionuclide therapy.* Eur J Nucl Med Mol Imaging, 2021. **48**(9): p. 2680-2682.
48. Aerts, A., et al., *EANM position paper on the role of radiobiology in nuclear medicine.* European Journal of Nuclear Medicine and Molecular Imaging, 2021. **48**(11): p. 3365-3377.
49. Terry, S.Y.A., et al., *Call to arms: need for radiobiology in molecular radionuclide therapy.* Eur J Nucl Med Mol Imaging, 2019. **46**(8): p. 1588-1590.
50. Andreassen, C.N., et al., *Radiogenomics - current status, challenges and future directions.* Cancer Lett, 2016. **382**(1): p. 127-136.
51. Leszczynski, D., *Radiation proteomics: a brief overview.* Proteomics, 2014. **14**(4-5): p. 481-8.
52. Vostrikova, S.M., A.B. Grinev, and V.G. Gogvadze, *Reactive Oxygen Species and Antioxidants in Carcinogenesis and Tumor Therapy.* Biochemistry (Mosc), 2020. **85**(10): p. 1254-1266.
53. Lawenda, B.D., et al., *Should supplemental antioxidant administration be avoided during chemotherapy and radiation therapy?* J Natl Cancer Inst, 2008. **100**(11): p. 773-83.
54. Prasad, K.N., et al., *Pros and cons of antioxidant use during radiation therapy.* Cancer Treat Rev, 2002. **28**(2): p. 79-91.
55. Nakayama, A., et al., *Systematic review: generating evidence-based guidelines on the concurrent use of dietary antioxidants and chemotherapy or radiotherapy.* Cancer Invest, 2011. **29**(10): p. 655-67.
56. Sayin, V.I., et al., *Antioxidants accelerate lung cancer progression in mice.* Sci Transl Med, 2014. **6**(221): p. 221ra15.
57. Le Gal, K., et al., *Antioxidants can increase melanoma metastasis in mice.* Sci Transl Med, 2015. **7**(308): p. 308re8.
58. Borek, C., *Antioxidants and radiation therapy.* J Nutr, 2004. **134**(11): p. 3207s-3209s.
59. Åkerstrom, B., et al., *The lipocalin alpha1-microglobulin has radical scavenging activity.* J Biol Chem, 2007. **282**(43): p. 31493-503.
60. Åkerstrom, B. and M. Gram, *A1M, an extravascular tissue cleaning and housekeeping protein.* Free Radic Biol Med, 2014. **74**: p. 274-82.

61. Allhorn, M., et al., *Processing of the lipocalin alpha(1)-microglobulin by hemoglobin induces heme-binding and heme-degradation properties.* Blood, 2002. **99**(6): p. 1894-901.
62. Kristiansson, A., et al., *Human radical scavenger α(1)-microglobulin protects against hemolysis in vitro and α(1)-microglobulin knockout mice exhibit a macrocytic anemia phenotype.* Free Radic Biol Med, 2021. **162**: p. 149-159.
63. Olsson, M.G., et al., *Up-regulation of A1M/alpha1-microglobulin in skin by heme and reactive oxygen species gives protection from oxidative damage.* PLoS One, 2011. **6**(11): p. e27505.
64. Rutardottir, S., et al., *The cysteine 34 residue of A1M/alpha1-microglobulin is essential for protection of irradiated cell cultures and reduction of carbonyl groups.* Free Radic Res, 2013. **47**(6-7): p. 541-50.
65. Olsson, M.G., et al., *The radical-binding lipocalin A1M binds to a Complex I subunit and protects mitochondrial structure and function.* Antioxid Redox Signal, 2013. **18**(16): p. 2017-28.
66. Bergwik, J., et al., *Structure, Functions, and Physiological Roles of the Lipocalin α(1)-Microglobulin (A1M).* Frontiers in physiology, 2021. **12**: p. 645650-645650.
67. DeMars, D.D., et al., *Simultaneous measurement of total and IgA-conjugated alpha 1-microglobulin by a combined immunoenzyme/immunoradiometric assay technique.* Clin Chem, 1989. **35**(5): p. 766-72.
68. Tejler, L., et al., *Production of protein HC by human fetal liver explants.* Biochim Biophys Acta, 1978. **542**(3): p. 506-14.
69. Nordberg, J., et al., *Quantitative and qualitative evaluation of plasma and urine alpha1-microglobulin in healthy donors and patients with different haemolytic disorders and haemochromatosis.* Clin Chim Acta, 2007. **386**(1-2): p. 31-7.
70. Ahlstedt, J., et al., *Human Anti-Oxidation Protein A1M—A Potential Kidney Protection Agent in Peptide Receptor Radionuclide Therapy.* International Journal of Molecular Sciences, 2015. **16**(12): p. 30309-30320.
71. Kristiansson, A., et al., *Kidney Protection with the Radical Scavenger α(1)-Microglobulin (A1M) during Peptide Receptor Radionuclide and Radioligand Therapy.* Antioxidants (Basel), 2021. **10**(8).
72. Olsson, M.G., et al., *Bystander cell death and stress response is inhibited by the radical scavenger α(1)-microglobulin in irradiated cell cultures.* Radiat Res, 2010. **174**(5): p. 590-600.
73. Kristiansson, A., et al., *Protection of Kidney Function with Human Antioxidation Protein α(1)-Microglobulin in a Mouse (177)Lu-DOTATATE Radiation Therapy Model.* Antioxid Redox Signal, 2019. **30**(14): p. 1746-1759.
74. Kristiansson, A., et al., *(177)Lu-PSMA-617 Therapy in Mice, with or without the Antioxidant α(1)-Microglobulin (A1M), Including Kidney*

Damage Assessment Using (99m)Tc-MAG3 Imaging. Biomolecules, 2021. **11**(2).
75. Molitoris, B.A., et al., *Technology Insight: biomarker development in acute kidney injury--what can we anticipate?* Nat Clin Pract Nephrol, 2008. **4**(3): p. 154-65.
76. Ferguson, M.A. and S.S. Waikar, *Established and emerging markers of kidney function.* Clin Chem, 2012. **58**(4): p. 680-9.
77. Bagshaw, S.M. and R. Bellomo, *Cystatin C in acute kidney injury.* Curr Opin Crit Care, 2010. **16**(6): p. 533-9.
78. Cirillo, M., P. Anastasio, and N.G. De Santo, *Relationship of gender, age, and body mass index to errors in predicted kidney function.* Nephrol Dial Transplant, 2005. **20**(9): p. 1791-8.
79. Filler, G., et al., *Cystatin C as a marker of GFR--history, indications, and future research.* Clin Biochem, 2005. **38**(1): p. 1-8.
80. Kawamura, J., S. Hosokawa, and O. Yoshida, *Renal function studies using 99mTc-dimercaptosuccinic acid.* Clin Nucl Med, 1979. **4**(1): p. 39-46.
81. Taylor, A., Jr., D. Eshima, and N. Alazraki, *99mTc-MAG3, a new renal imaging agent: preliminary results in patients.* Eur J Nucl Med, 1987. **12**(10): p. 510-4.
82. Vaidya, V.S., M.A. Ferguson, and J.V. Bonventre, *Biomarkers of acute kidney injury.* Annu Rev Pharmacol Toxicol, 2008. **48**: p. 463-93.
83. Schrezenmeier, E.V., et al., *Biomarkers in acute kidney injury - pathophysiological basis and clinical performance.* Acta Physiol (Oxf), 2017. **219**(3): p. 554-572.
84. Ye, Z., et al., *Correlation and Diagnostic Value of Serum Cys-C, RBP4, and NGAL with the Condition of Patients with Traumatic Acute Kidney Injury.* Evidence-Based Complementary and Alternative Medicine, 2021. **2021**: p. 4990941.
85. Karmakova, T., et al., *Kidney Injury Molecule 1 (KIM-1): a Multifunctional Glycoprotein and Biological Marker (Review).* Sovrem Tekhnologii Med, 2021. **13**(3): p. 64-78.
86. Norden, A.G., M. Lapsley, and R.J. Unwin, *Urine retinol-binding protein 4: a functional biomarker of the proximal renal tubule.* Adv Clin Chem, 2014. **63**: p. 85-122.
87. Dalmo, J., et al., *Evaluation of retinol binding protein 4 and carbamoylated haemoglobin as potential renal toxicity biomarkers in adult mice treated with (177)Lu-octreotate.* EJNMMI Res, 2014. **4**(1): p. 59.
88. Schüler, E., et al., *Distinct microRNA expression profiles in mouse renal cortical tissue after 177Lu-octreotate administration.* PLoS One, 2014. **9**(11): p. e112645.
89. Schüler, E., et al., *Time- and dose rate-related effects of internal (177)Lu exposure on gene expression in mouse kidney tissue.* Nucl Med Biol, 2014. **41**(10): p. 825-32.

90. Schüler, E., et al., *Transcriptional response of kidney tissue after 177Lu-octreotate administration in mice.* Nucl Med Biol, 2014. **41**(3): p. 238-47.
91. Schüler E, D.J., Larsson M, Parris TZ, Helou K, Forssell-Aronsson E, *Proteomics and functional analysis for the assessment of radiation induced response after 177Lu-octreotate administration in mice*, U.o. Gothenburg, Editor. 2014.
92. Schüler, E., et al., *Potential Biomarkers for Radiation-Induced Renal Toxicity following 177Lu-Octreotate Administration in Mice.* PLoS One, 2015. **10**(8): p. e0136204.
93. Åkerström, B., et al., *rA1M-035, a Physicochemically Improved Human Recombinant α(1)-Microglobulin, Has Therapeutic Effects in Rhabdomyolysis-Induced Acute Kidney Injury.* Antioxid Redox Signal, 2019. **30**(4): p. 489-504.
94. Kölby, L., et al., *A transplantable human carcinoid as model for somatostatin receptor-mediated and amine transporter-mediated radionuclide uptake.* Am J Pathol, 2001. **158**(2): p. 745-55.
95. Johanson, V., et al., *A transplantable human medullary thyroid carcinoma as a model for RET tyrosine kinase-driven tumorigenesis.* Endocr Relat Cancer, 2007. **14**(2): p. 433-44.
96. Bolch, W.E., et al., *MIRD pamphlet No. 21: a generalized schema for radiopharmaceutical dosimetry--standardization of nomenclature.* J Nucl Med, 2009. **50**(3): p. 477-84.
97. Miller, W.H., et al., *Evaluation of beta-absorbed fractions in a mouse model for 90Y, 188Re, 166Ho, 149Pm, 64Cu, and 177Lu radionuclides.* Cancer Biother Radiopharm, 2005. **20**(4): p. 436-49.
98. Schüler, E., A. Österlund, and E. Forssell-Aronsson, *The amount of injected 177Lu-octreotate strongly influences biodistribution and dosimetry in C57BL/6N mice.* Acta Oncol, 2016. **55**(1): p. 68-76.
99. Livak, K.J. and T.D. Schmittgen, *Analysis of relative gene expression data using real-time quantitative PCR and the 2(-Delta Delta C(T)) Method.* Methods, 2001. **25**(4): p. 402-8.
100. Dalmo, J., et al., *Biodistribution of 177Lu-octreotate and 111In-minigastrin in female nude mice transplanted with human medullary thyroid carcinoma GOT2.* Oncol Rep, 2012. **27**(1): p. 174-81.
101. Kölby, L., et al., *Successful receptor-mediated radiation therapy of xenografted human midgut carcinoid tumour.* Br J Cancer, 2005. **93**(10): p. 1144-51.
102. Dizdar, L., et al., *Preclinical assesement of survivin and XIAP as prognostic biomarkers and therapeutic targets in gastroenteropancreatic neuroendocrine neoplasia.* Oncotarget, 2017. **8**(5): p. 8369-8382.
103. Hanif, A., et al., *Exploring the role of survivin in neuroendocrine neoplasms.* Oncotarget, 2020. **11**(23): p. 2246-2258.
104. Werner, T.A., et al., *Survivin and XIAP: two valuable biomarkers in medullary thyroid carcinoma.* Br J Cancer, 2016. **114**(4): p. 427-34.

105. Li, S., et al., *Identification and Validation of Candidate Radiation-responsive Genes for Human Biodosimetr.* Biomed Environ Sci, 2017. **30**(11): p. 834-840.
106. Kultova, G., et al., *The hunt for radiation biomarkers: current situation.* Int J Radiat Biol, 2020. **96**(3): p. 370-382.
107. Marchetti, F., et al., *Candidate protein biodosimeters of human exposure to ionizing radiation.* Int J Radiat Biol, 2006. **82**(9): p. 605-39.
108. Haider, S. and R. Pal, *Integrated analysis of transcriptomic and proteomic data.* Current genomics, 2013. **14**(2): p. 91-110.
109. Åkerström, B., et al., *alpha(1)-Microglobulin: a yellow-brown lipocalin.* Biochim Biophys Acta, 2000. **1482**(1-2): p. 172-84.
110. Wester, L., et al., *Receptor for alpha1-microglobulin on T lymphocytes: inhibition of antigen-induced interleukin-2 production.* Scand J Immunol, 1998. **48**(1): p. 1-7.
111. Fernandez-Luna, J.L., F. Leyva-Cobian, and F. Mollinedo, *Identification of the protein HC receptor.* FEBS Lett, 1988. **236**(2): p. 471-4.
112. Huang, J., et al., *Serum amyloid A1 as a biomarker for radiation dose estimation and lethality prediction in irradiated mouse.* Ann Transl Med, 2019. **7**(23): p. 715.
113. Chen, C., et al., *A proteomic analysis of murine bone marrow and its response to ionizing radiation.* Proteomics, 2005. **5**(16): p. 4254-63.
114. Magić, Z., et al., *Ionizing radiation-induced expression of the genes associated with the acute response to injury in the rat.* Radiat Res, 1995. **143**(2): p. 187-93.
115. Andersen, C.B.F., et al., *Haptoglobin.* Antioxid Redox Signal, 2017. **26**(14): p. 814-831.
116. Rolleman, E.J., et al., *Long-term toxicity of [(177)Lu-DOTA (0),Tyr (3)]octreotate in rats.* Eur J Nucl Med Mol Imaging, 2007. **34**(2): p. 219-27.
117. Forrer, F., et al., *From outside to inside? Dose-dependent renal tubular damage after high-dose peptide receptor radionuclide therapy in rats measured with in vivo (99m)Tc-DMSA-SPECT and molecular imaging.* Cancer Biother Radiopharm, 2007. **22**(1): p. 40-9.